Inorganic Chemistry

Article

pubs.acs.org/IC

# Rhenium and Technetium-oxo Complexes with Thioamide Derivatives of Pyridylhydrazine Bifunctional Chelators Conjugated to the Tumour Targeting Peptides Octreotate and Cyclic-RGDfK

Andrea J. North,[†] John A. Karas,[†] Michelle T. Ma,[‡] Philip J. Blower,[‡] Uwe Ackermann,[§] Jonathan M. White,[†] and Paul S. Donnelly*[,†]

[†]The School of Chemistry and Bio21 Molecular Science and Biotechnology Institute, University of Melbourne, 3010, Victorria, Australia

[‡]Division of Imaging Sciences and Biomedical Engineering, King's College London, Fourth Floor Lambeth Wing, St Thomas' Hospital, London SE1 7EH, U.K.

[§]Department of Molecular Imaging and Therapy, Department of Medicine, University of Melbourne, Austin Health, Studley Road, Heidelberg, Victoria 3010, Australia

Supporting Information

**ABSTRACT:** This research aimed to develop new tumor targeted theranostic agents taking advantage of the similarities in coordination chemistry between technetium and rhenium. A $\gamma$-emitting radioactive isotope of technetium is commonly used in diagnostic imaging, and there are two $\beta^-$ emitting radioactive isotopes of rhenium that have the potential to be of use in radiotherapy. Variants of the 6-hydrazinonicotinamide (HYNIC) bifunctional ligands have been prepared by appending thioamide functional groups to 6-hydrazinonicotinamide to form pyridylthiosemicarbazide ligands (SHYNIC). The new bidentate ligands were conjugated to the tumor targeting peptides Tyr$^3$-octreotate and cyclic-RGD. The new ligands and conjugates were used to prepare well-defined $\{M{=}O\}^{3+}$ complexes (where M = $^{99m}$Tc or $^{nat}$Re or $^{188}$Re) that feature two targeting peptides attached to the single metal ion. These new SHYNIC ligands are capable of forming well-defined rhenium and technetium complexes and offer the possibility of using the $^{99m}$Tc imaging and $^{188/186}$Re therapeutic matched pairs.

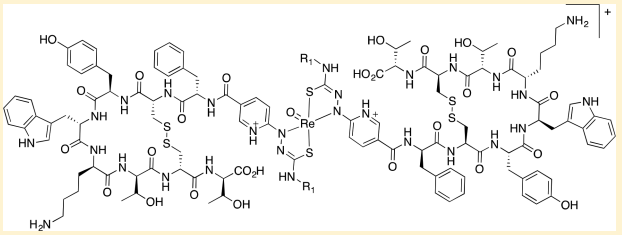

## INTRODUCTION

The technetium-99m isotope has excellent properties for detection with single photon emission computed tomography (SPECT) due to its low energy and nonparticulate gamma-ray emission ($t_{1/2}$ = 6.01 h, $E_{max}$ = 141 keV $\gamma$-ray emission, $\lambda$ < 10 pm). Despite recent concerns over production related shortages of technetium-99m and the advent of positron emission tomography technetium-99m retains its importance to nuclear medicine to the extent that the isotope is used in over 80% of nuclear imaging procedures worldwide.[1] The heavier third row Group VII congener, rhenium, has an ionic radius similar to technetium due to the lanthanide contraction. Technetium and rhenium display similar coordination chemistry often resulting in essentially isostructural technetium and rhenium complexes. It is common for technetium and rhenium complexes to be essentially isostructural. There are two isotopes of rhenium that are of potential use in targeted radiotherapeutics, rhenium-186 ($t_{1/2}$ = 89.3 h, $E_{max}$ = 1.07 MeV $\beta^-$ particle emission, 137 keV $\gamma$-ray emission) and rhenium-188 (($t_{1/2}$ = 16.9 h, $E_{max}$ = 2.12 MeV $\beta^-$ particle emission, 155 keV $\gamma$-ray emission). The similar coordination chemistry of technetium and rhenium offers the possibility of using their radioisotopes as an imaging ($^{99m}$Tc) and therapeutic ($^{186/188}$Re) matched pair using a single targeted ligand to form essentially isostructural complexes.[2−6]

One approach to targeted imaging and therapy is to incorporate appropriate metal radionuclides into coordination complexes that are attached to biological targeting vectors such as tumor targeting peptides, antibodies or antibody fragments. Peptides that feature the −RGD- (arginine-glycine-aspartic acid) fibronectin fragment such as the cyclic-RGDfK pentapeptide (cRGDfK) bind to $\alpha_v\beta_3$ integrin receptors that are overexpressed in certain invasive tumors including osteosarcomas, glioblastoma, melanomas, and breast cancer, and can be used to selectively target tumor cells.[7−16] Metabolically stabilized somatostatin analogues such as octreotide and octreotate bind to somatostatin subtype 2 receptors (sstr2) that are overexpressed in many types of neuroendocrine tumors compared to relatively low levels of expression in other tissues and organs.[17−21]

Tumor targeting technetium based imaging agents can be prepared using 6-hydrazinonicotinamide (HYNIC) derivatives conjugated to targeting molecules as ligands to form

**Received:** May 17, 2017
**Published:** August 2, 2017

  

DOI: 10.1021/acs.inorgchem.7b01247
Inorg. Chem. 2017, 56, 9725−9741

technetium(III) diazenido complexes.[22−31] The HYNIC ligand forms remarkably stable technetium complexes, and manipulation of the carboxylate functional group to attach a variety of targeting molecules is generally straightforward. HYNIC binds to technetium through the terminal hydrazine nitrogen but probably forms bidentate complexes through coordination to the pyridyl nitrogen.[29,32] In all the crystallographically characterized technetium and rhenium complexes with one or more HYNIC-like ligands, such as 2-hydrazinopyridine, the pyridyl nitrogen is also coordinated to the metal center.[33] A variety of coligands such as tricine, nicotinic acid, EDDA, and phosphines (TPPTS, TPPDS, TPPMS = tri/bi/sodium triphenylphosphine tri/di/monosulfonate) are required to complete the coordination sphere and stabilize the metal oxidation state, and this leads to a high degree of uncertainty in the exact nature of the primary coordination sphere as well as challenges in ensuring structural homogeneity in the formulated product. Variation of the coligand can modify the in vivo metabolism and excretion.[34] A well-established "ternary ligand system" involves combining the HYNIC ligand with tetradentate tricine and monodentate trisodium 3,3′,3″-phosphanetriyltris(benzenesulfonate) (TPPTS) coligands, but the possibility of forming multiple isomers adds complications.[33,35−39]

Despite the superficial similarities in coordination chemistry between technetium and rhenium extrapolation of the HYNIC strategy to radioactive rhenium isotopes is challenging presumably due to their differences in kinetic lability and redox chemistry.[33] Some of the difficulty in isolating pure Re-HYNIC-peptide conjugates can be understood by considering the reaction of $[ReO_4]^-$ with 2-hydrazinopyridine (used as model for HYNIC).[33,40] This reaction results in relatively complex coordination chemistry due to the ability of the pyridylhydrazine derived ligands to coordinate as either monodentate or bidentate ligands and the existence of protic equilibria as well as the formation of complexes where two pyridylhydrazine derived units are coordinated to the rhenium (Figure 1).[26,33,40−43]

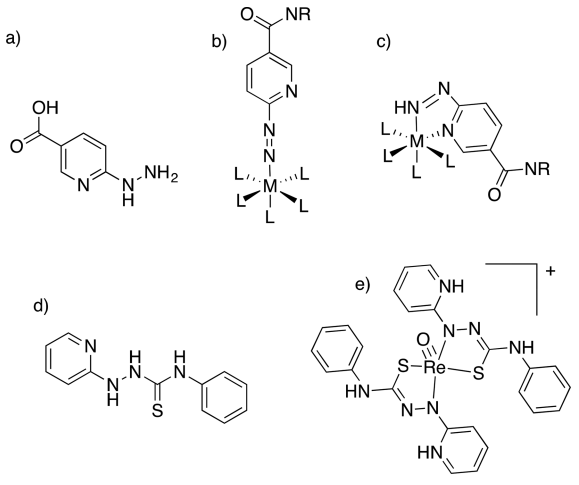


**Figure 1.** (a) 6-Hydrazinonicotinic acid. (b) Metal complex (M = Tc or Re) with 6-hydrazinonicotinimide (HYNIC) acting as a monodentate ligand. It is necessary to complete the coordination sphere with coligands (L). (c) Metal complex (M = Tc or Re) with 6-hydrazinonicotinimide (HYNIC) acting as a bidentate ligand. (d) Pyridylphenylthiocarbazide (SHYNIC) ligand. (e) $Re^V$-oxo complex featuring two SHYNIC ligands.[44]

Modification of the terminal hydrazinic nitrogen of hydrazinopyridine to incorporate an additional thiourea functional group results in a ligand system that is capable of forming well-defined, very stable complexes with $\{Re^VO\}^{3+}$ cores while retaining the bioconjugation possibilities well established for HYNIC.[44,45] A preliminary communication reported the structural characterization of a $Re^V$-oxo complex featuring two pyridylphenylthiocarbazide (*S*HYNIC) ligands (Figure 1).[44] In this manuscript we extend this concept by synthesizing a family of different substituted pyridylthiosemicarbazide ligands with carboxylate or ester functional groups that were used to tether octreotate and cyclic-RGD peptides to the ligands. The new ligands were used to prepare $\{MO\}^{3+}$ complexes (where M = Tc or Re) that feature two targeting peptides attached to the single metal ion. These modified HYNIC ligands are capable of forming well-defined rhenium and technetium complexes and offer the possibility of using the two radionuclides as imaging and therapeutic matched pairs.

## RESULTS AND DISCUSSION

**Synthesis of $H_2L^{1-4}$, and Their Ester Derivatives, $H_2L^{1-4}(OMe)$ and $\{ReO\}^{3+}$ Complexes.** Synthesis of 6-hydrazinonictonic acid (HYNIC), **2**, required treatment of 6-chloronicotinic acid (**1**) with aqueous hydrazine.[47] Ligands $H_2L^1$ to $H_2L^4$ were prepared by reaction of either the ethyl, *tert*-butyl, phenyl, or nitrophenyl isothiocyanate with 6-hydrazinonictonic acid (**1**) in anhydrous *N*,*N*-dimethylacetamide (DMA) (Scheme 1).

The rhenium complexes of the methyl ester derivatives of $H_2L^{1-3}$ complexes, $[ReO(HL^{1-3}(OMe))_2]^+$, can be prepared by reaction of the either *trans*-$[ReOCl_3(PPh_3)_2]$ or $[tBu_4N][ReOCl_4]$ with the two equivalents of ligand (Scheme 2). The IR spectra for the three complexes, $[ReO(H_2L^{1-3}(OMe))_2]^+$, display medium intensity bands at $\bar{\nu}$ 960−963 $cm^{-1}$ characteristic of Re═O stretches.[48] Bands, which occur between $\bar{\nu}$ 1553 and 1557 $cm^{-1}$ due to carbonyl stretching of the ester functional group, shift approximately 150 $cm^{-1}$ lower in energy when compared to the metal-free ligands.

Analysis of the complexes by $^1H$ NMR data reveals that the two coordinated ligands are magnetically equivalent, with three resonances at $\delta$ 8.63, 8.25, and 7.86 ppm corresponding to the six pyridinyl C*H* protons for $[ReO(HL^1(OMe))_2]^+$, and similar resonances for the phenyl and *tert*-butyl derivatives. The pyridine proton which is closest to the rhenium ion shifts from $\delta$ 6.55 ppm in free ligand to $\delta$ 7.86 ppm in the complex. The methyl ester functional group gives rise to singlets at $\delta$ 3.89 (DMSO-$d_6$), 3.86 ($CHCl_3$-*d*), and 3.92 (DMSO-$d_6$) for complexes $[ReO((HL^{1,2,3})(OMe))_2]^+$ respectively. The $[ReO(HL^1(OMe))_2]^+$ complex was stable to cysteine and histidine challenge experiments with very little decomposition evident (<5%), as detected by analysis by HPLC and UV/vis spectroscopy, when incubated at 37 °C for 24 h in the presence of a 100-fold excess of cysteine and histidine.

Red crystals of $[ReO(HL^1(OMe))_2]CF_3CO_2$ suitable for X-ray crystallographic analysis were obtained by evaporation of a solution of the compound that had been purified by semipreparative HPLC using an aqueous/$CH_3CN$ mobile phase with 0.1% trifluoracetic acid (Figure 2a). The compound crystallizes in the triclinic space group, $P\bar{1}$, and the rhenium ion is in a distorted square pyramidal environment with the oxo group in the apical position relative to the pseudo basal plane of two five-membered chelate rings. Each thiocarbahydrazide functional group is doubly deprotonated and serves as a


DOI: 10.1021/acs.inorgchem.7b01247
*Inorg. Chem.* 2017, 56, 9725−9741

**Scheme 1. Synthesis of Ligands $H_2L^1$–$H_2L^4$ and Their Methyl Ester Derivatives $H_2L^1(OMe)$–$H_2L^4(OMe)$**

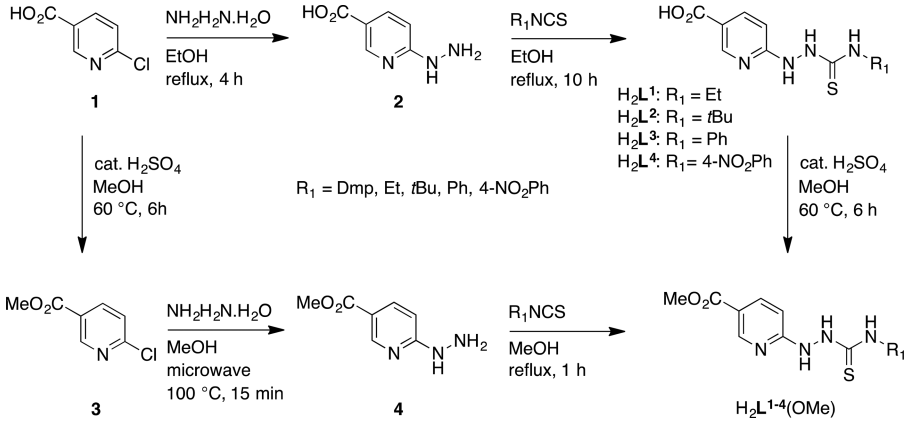


**Scheme 2. Synthesis of Rhenium Complexes $[ReO(HL^{1-3})(OMe))_2]^+$**

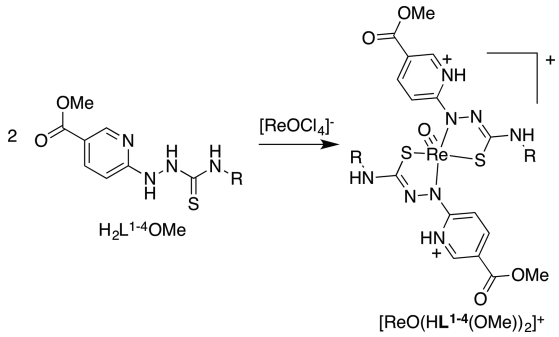


dianionic ligand fragment and a *N,N/S,S trans* configuration about the Re-oxo. The selective formation of the *N,N/S,S trans* geometric isomer presumably reflects a strong "*trans* effect", although steric requirements may also play some role.[49−51] Protonation of the pyridyl nitrogen atom in each ligand results in each ligand having a single negative charge and resulting an overall monocationic complex. The two pyridinium protons and the hydrogen atoms of the ethylamino functional group are involved in hydrogen bonds interactions leading to a hydrogen bonded centrosymmetric dimer (Figure 2b) with the two remaining H-bond donors capped by water molecules.

The Re−O1 bond distance (1.679(3) Å) is typical for five-coordinate, rhenium(V)-monooxo complexes and consistent with IR spectroscopy (Re═O, $\bar{\nu}$ 963 $cm^{-1}$).[52−55] The N2−C6 and N6−C14 bond lengths (1.287(6) Å) are significantly shorter than the other bonds within the chelate ring suggesting significant $sp^2$ hybridized C═N bond character. The Re−N bond distances average 2.05 Å and are marginally shorter than typical Re−N bonds (ca. 2.15−2.18 Å) suggesting some degree of multiple bond character.[51,56] The Re−N1−N2 and Re−N5−N6 bond angles average 124°, suggesting an approximately $sp^2$ hybridized nitrogen. The Re−S bond distances average 2.29 Å and are similar to the Re−S bond distances in rhenium(V) complexes with amino thiolate ligands and Re−S bond distances in rhenium complexes with thiosemicarbazonato ligands.[51,57,58]

The potential of the substituted pyridylthiosemicarbazide (SHYNIC) ligands $H_2L^{1-4}$ to be modified with amino acids using standard solid phase peptide synthesis techniques was first accomplished by attaching L-lysine to $H_2L^1$ to give $H_2L^1$(Lys). The doubly N-protected lysine derivative, $N_\alpha$-*t*Boc-$N_\varepsilon$-Fmoc-L-Lys, was immobilized on chlorotrityl resin, and the $N_\varepsilon$-Fmoc group was removed by treatment with piperidine. The ligand, $H_2L^1$, was added to the resin in a mixture of DMF followed by the coupling agent HATU (HATU = 1-[bis(dimethylamino)methylene]-1*H*-1,2,3-triazolo[4,5-b]-pyridinium-3-oxid hexafluorophosphate) in the presence of *N,N*-diisopropylethylamine (DIPEA). The product was cleaved from the resin using trifluoroacetic acid that also resulted in the deprotection of the $N_\alpha$-*t*-butoxycarbonyl group (Scheme 3). This lysine amino acid conjugate provides an amino acid with an appended chelator, which with appropriate protecting groups, could be incorporated into biological targeting molecules with total site specificity via solid-phase peptide synthesis.[59−63]

The rhenium complex, $[ReO(HL^1(Lys))_2]^+$, was prepared by adding either *trans*-$[ReOCl_3(PPh_3)_2]$ or $[t\text{Bu}N][ReOCl_4]$ suspended in DMF to the reaction mixture, while the ligand remained immobilized on the resin. Performing the complexation while the ligand remained immobilized on the resin and with the amino group still protected ensured that the functional groups of the lysine did not complicate the coordination chemistry. When green *trans*-$[ReOCl_3(PPh_3)_2]$ is used as the starting material the green colored suspension gradually changes to colorless, and the resin beads turn dark red indicative of the formation of $[ReO(HL^1(Lys))_2]^+$. After being stirred at room temperature, the resin was washed with dimethylformamide and dichloromethane and cleaved off the resin with a 10% trifluoroacetic acid/dichloromethane mixture (Scheme 3). Analysis of $[ReO(HL^1(Lys))_2]^+$ complex by electrospray ionization mass spectrometry (ESI-MS) reveals the expected peaks. Analysis by $^1H$ NMR shows the singlet attributed to the aromatic proton on the pyridine ring (py$H^2$) shifts upon coordination to the metal center from $\delta$ 8.48 in $H_2L^1$(Lys) to 8.58 ppm in $[ReO(HL^1(Lys))_2]^+$. The four downfield $^{13}C\{^1H\}$ NMR signals in $[ReO(HL^1(Lys))2]^+$, 173.0 ($CO_2H$), 169.0 (N═CS), 165.4 (CONH), and 163.6 (py$C^6$), were assigned using HSQC and HMBC techniques.

**Synthesis of Peptide-Conjugated Ligands, $H_2L^{1-3}$(cRGDfK) and $H_2L^{1-3}$(Tyr$^3$-Octreotate), and Corresponding Rhenium Complexes $[ReO((HL^{1-3})(cRGDfK))_2]$ and $[ReO((HL^{1-3})(Tyr^3\text{-Octreotate}))_2]$.** The cyclic pentapeptide, cRGDfK, was prepared using standard solid phase peptide synthesis techniques with Fmoc (Fmoc = 9-fluorenylmethyloxycarbonyl) protected amino acids, using HATU/DIPEA coupling methodology on chlorotrityl resin. The Fmoc protecting groups were removed with 20% piperidine in


DOI: 10.1021/acs.inorgchem.7b01247
*Inorg. Chem.* 2017, 56, 9725−9741

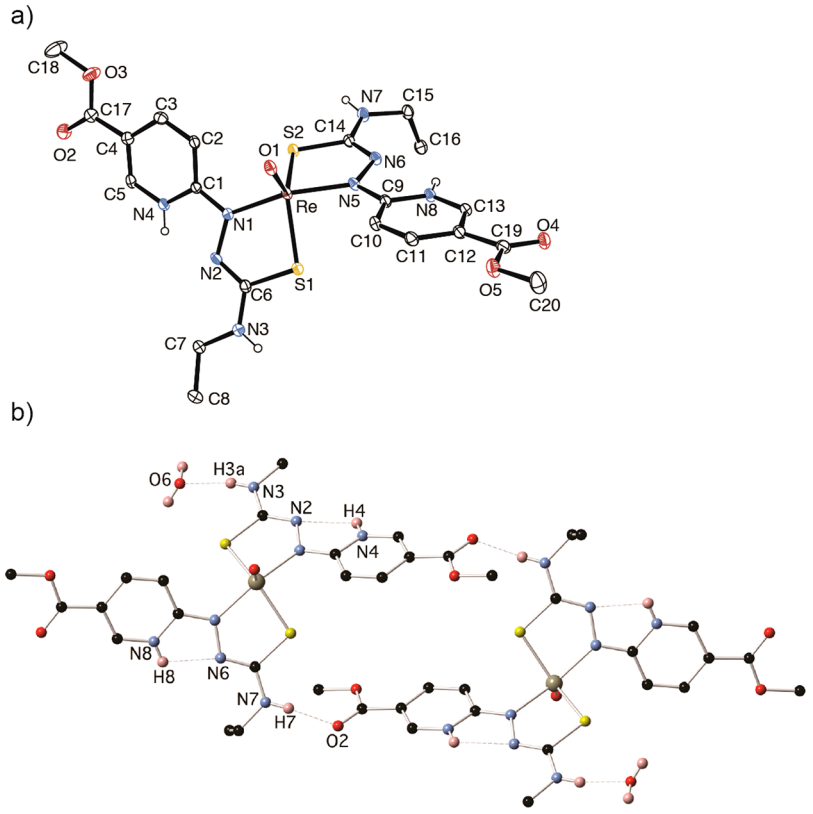


**Figure 2.** (a) ORTEP representation of $[ReO(HL^1(OMe))_2]^+$ (50% probability ellipsoids). The trifluoroacetate counterion and hydrogen atoms (except those bound to nitrogen) are omitted. (b) Representation of hydrogen bonded centrosymmetric dimer with the two remaining H-bond donors capped by water molecules.

**Table 1. Selected Bond Lengths (Å) and Angles (deg) for the Rhenium Complex for $[ReO(HL^1(OMe))_2]CF_3CO_2$[a]**

| | | | | | |
|---|---|---|---|---|---|
| Bond Lengths | | | | | |
| Re–O(1) | 1.679(3) | Re–S(1) | 2.2820(11) | Re–S(2) | 2.2917(11) |
| N(1)–C(1) | 1.350(6) | Re–N(1) | 2.049(4) | Re–N(5) | 2.050(4) |
| C(6)–N(3) | 1.343(6) | N(1)–N(2) | 1.422(5) | N(5)–N(6) | 1.418(5) |
| C(14)–N(7) | 1.350(6) | N(2)–C(6) | 1.287(6) | N(6)–C(14) | 1.287(6) |
| N(5)–C(9) | 1.356(6) | C(6)–S(1) | 1.784(5) | C(14)–S(2) | 1.769(4) |
| Bond Angles | | | | | |
| O(1)–Re–S(1) | 115.44(11) | N(1)–Re–S(1) | 80.74(11) | | |
| O(1)–Re–S(2) | 116.75(11) | N(5)–Re–S(2) | 80.23(11) | | |
| O(1)–Re–N(1) | 101.73(15) | N(5)–Re–S(1) | 89.71(11) | | |
| O(1)–Re–N(5) | 102.61(15) | N(1)–Re–S(2) | 87.98(11) | | |
| N(1)–Re–N(5) | 155.64(15) | C(1)–N(1)–Re | 125.0(3) | | |
| S(1)–Re–S(2) | 127.80(4) | C(9)–N(5)–Re | 126.2(3) | | |
| Torsion Angles | | | | | |
| N(4)–C(1)–N(1)–Re | 169.5(3) | N(6)–C(14)–N(7)–C(15) | 13.8(7) | | |
| N(8)–C(9)–N(5)–Re | 173.3(3) | N(2)–C(6)–N(3)–C(7) | 5.1(7) | | |
| N(4)–C(1)–N(1)–N(2) | −10.5(6) | N(2)–C(6)–S(1)–Re | 3.7(4) | | |
| N(8)–C(9)–N(5)–N(6) | −7.8(6) | N(6)–C(14)–S(2)–Re | 4.1(4) | | |
| C(2)–C(1)–N(1)–N(2) | 167.1(4) | N(3)–C(6)–S(1)–Re | −174.7(3) | | |
| C(10)–C(9)–N(5)–N(6) | 168.4(4) | N(7)–C(14)–S(2)–Re | −175.1(3) | | |

[a]Trifluoroacetate counterion bond lengths and angles are not provided.

DMF on the solid phase, followed by cleavage from the resin and cyclization using a small modification of published procedures.[64] The ligands, $H_2L^{1-3}$, were conjugated to cRGDfK using standard peptide coupling conditions (HATU, DIPEA) to give $H_2L^{1-3}$(cRGDfK) (Scheme 4). The new conjugates were purified by semipreparative RP-HPLC and characterized by electrospray mass spectrometry and analytical HPLC. The reaction for the ethyl-SHYNIC derivative, $H_2L^1$(cRGDfK), resulted in a higher isolated yield (80%) than $H_2L^2$(cRGDfK) (24%) and $H_2L^3$(cRGDfK) (55%). Analysis of aqueous solutions of $H_2L^{1-3}$(cRGDfK) by RP-HPLC revealed no degradation over a 24 h.

The $\{ReO\}^{3+}$ complexes of $H_2L^{1-3}$(cRGDfK) were prepared by adding $[ReOCl_4]^-$ in DMF at ambient temperature followed



DOI: 10.1021/acs.inorgchem.7b01247
Inorg. Chem. 2017, 56, 9725−9741

**Table 2. Summary of Crystal Data and Structure Refinement for $[ReO(HL^1(OMe))_2]CF_3CO_2$[a]**

| data collection | compound details | data collection | compound details |
|---|---|---|---|
| empirical formula | $C_{20}H_{26}N_8O_5ReS_2.H_2O.CF_3CO_2$ | $V$ (Å$^3$) | 1551.05(13) |
| formula weight | 839.84 | $Z$ | 2 |
| crystal size (mm$^3$) | 0.26 × 0.10 × 0.022 | $D_{calc.}$ (Mg m$^{-3}$) | 1.797 |
| crystal system | triclinic | $\mu$ (mm$^{-1}$) | 9.599 |
| space group | $P\bar{1}$ | $F(000)$ | 828 |
| $T$ (K) | 130.00(10) | reflections measured | 10363 |
| $\lambda$ (Å) | 1.54184 | independent reflections | 5568 [$R_{int}$ = 0.0449] |
| $a$ (Å) | 10.9154(4) | final $R$ indices [$I > 2\sigma(I)$] | $R_1$ = 0.0329 |
| $b$ (Å) | 11.1201(6) | | $wR(F^2)$ = 0.0794 |
| $c$ (Å) | 13.2651(7) | final $R$ indices (all data) | $R_1$ = 0.0398 |
| $\alpha$ (deg) | 86.355(4) | | $wR(F^2)$ = 0.0831 |
| $\beta$ (deg) | 74.965(4) | goodness-of fit on $F^2$ | 1.027 |
| $\gamma$ (deg) | 87.273(4) | | |

[a]Crystals were grown from a concentrated solution of the complex in methanol.

**Scheme 3. "On-Resin" Formation of $H_2L^1$(Lys) and the Corresponding Rhenium-oxo Complex, $[ReO(HL^1(Lys))_2]^+$**

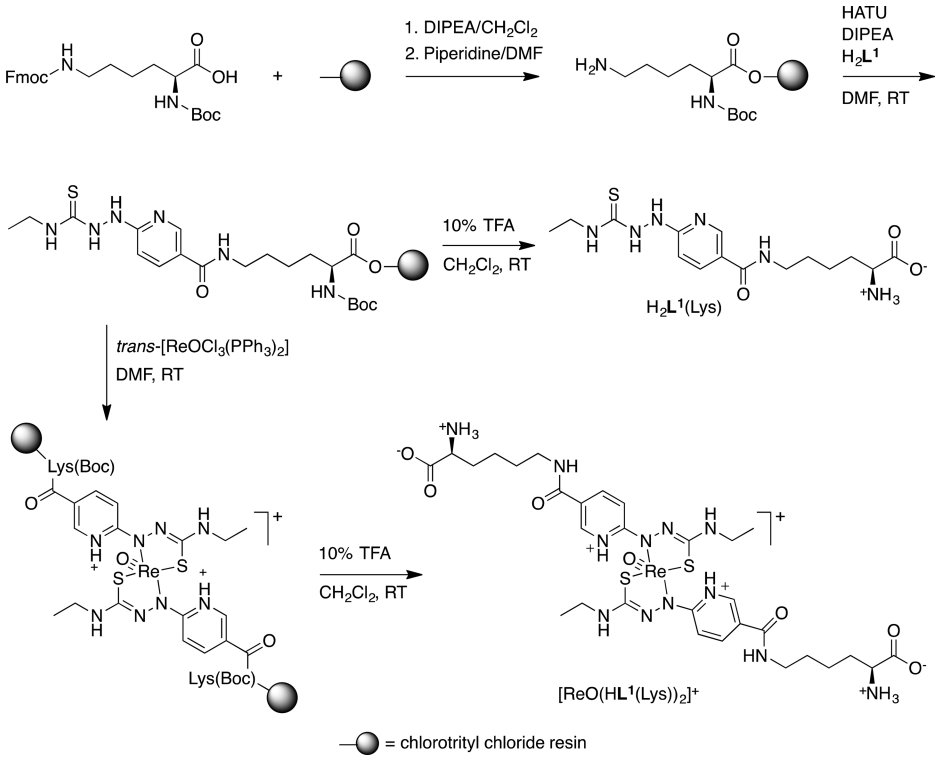


by isolation and purification using semipreparative RP-HPLC (Scheme 4). Analysis of the complexes by ESI-MS revealed the 2+ molecular ion peaks at $m/z$ 926.343, 954.372, and 974.371 for $[ReO(HL^1(cRGDfK))_2]^+$, $[ReO(HL^2(cRGDfK))_2]^+$, and $[ReO(HL^3(cRGDfK))_2]^+$ respectively.

An intramolecular disulfide bridge between the second and seventh cysteine residues in Tyr$^3$-octreotate improves the metabolic stability of the peptide, and this disulfide is often introduced by oxidation of the linear octapeptide with 2,2′-dithiodipyridine. Unfortunately the bioconjugation of ligands $H_2L^{1-3}$ to Tyr$^3$-octreotate was complicated by degradation of the pyridylthiocarbazide (SHYNIC) ligands ($H_2L^{1-3}$) in the presence of the two cysteine thiol containing residues in the linear peptide, leading to loss of $H_2S$ identified in the ESI-MS by a loss of 34 atomic mass units. This loss of $H_2S$ from the ligand was most prominent during reactions attempting intramolecular oxidation of thiol groups in the two cysteine residues. The loss of $H_2S$ results in the formation of a carbodiimide form of the SHYNIC ligands. The formation of carbodiimides from thioureas is well-known.[65] This degradation and loss of sulfur were not observed for RGD-based conjugates, suggesting that in the case of the octreotate conjugates, thiocarbazide-thiol-disulfide interchange/scrambling promotes the loss of $H_2S$ from the ligands (Scheme 5).

As conventional off-resin oxidative cyclization methodologies were inadequate for this synthesis, $H_2L^{1-3}$(Tyr$^3$-Oct) was prepared entirely on solid support, where intramolecular oxidation/cyclization preceded bioconjugation of $H_2L^{1-3}$. The eight-residue peptide was synthesized by sequential addition of the amino acid residues via solid-phase peptide synthesis, using acetamidomethyl (Acm) protected cysteine residues followed by in situ Acm removal and simultaneous disulfide bond formation using thallium(III) trifluoroacetate.[66] Following cyclization, the preactivated SHYNIC derivative ($H_2L^{1-3}$) is


DOI: 10.1021/acs.inorgchem.7b01247
Inorg. Chem. 2017, 56, 9725−9741

**Scheme 4. Synthesis of $H_2L^{1-3}$(cRGDfK) and $[ReO(HL^{1-3}(cRGDfK))_2]^+$**

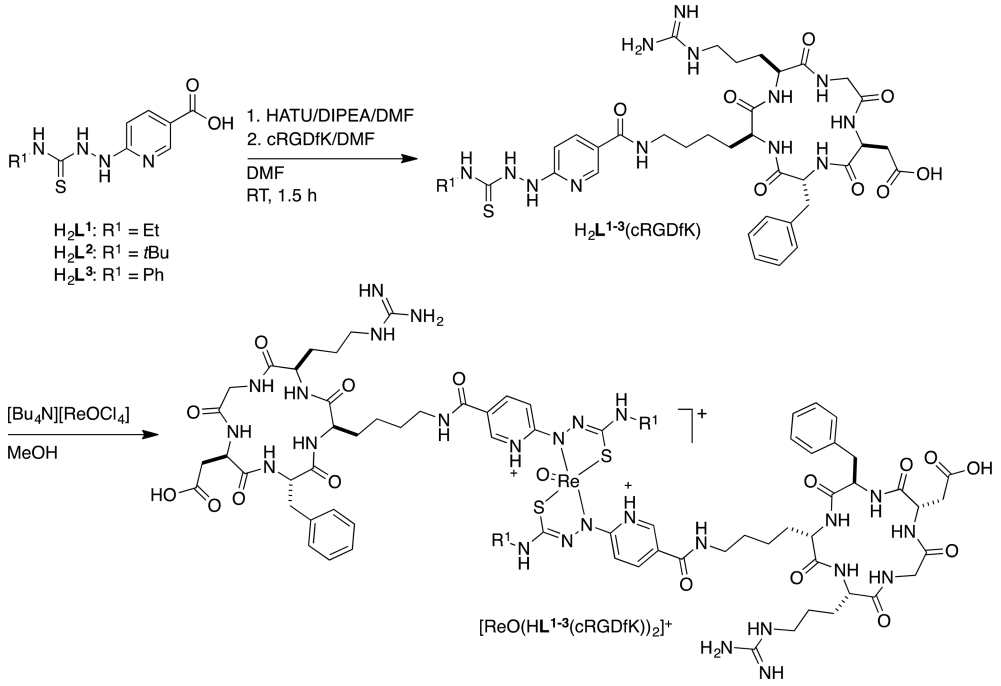


**Scheme 5. Suggested Mechanism for the Formation of a Carbodiimide from $H_2L^{1-3}$(Tyr³-Oct) Resulting in Loss of $H_2S$**

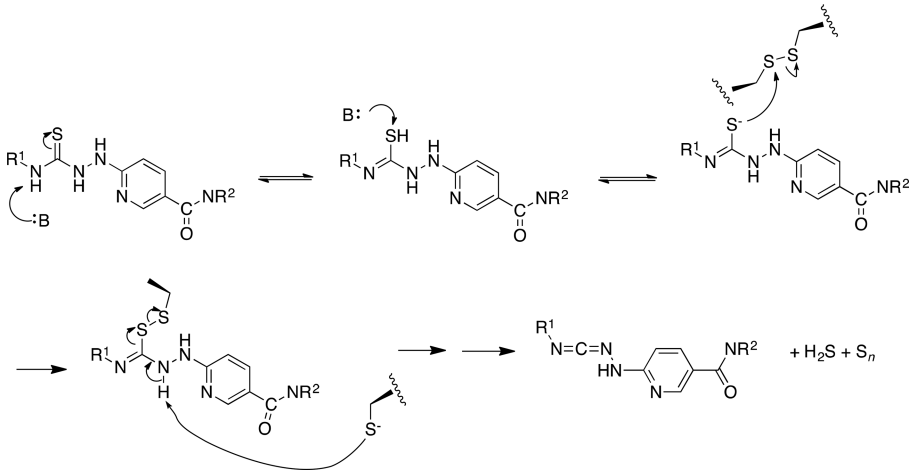


reacted at the deprotected D-phenylalanine N-terminus. Cleavage and deprotection of remaining protecting groups are achieved by treatment with trifluoracetic acid (Scheme 6).

The rhenium complexes of $H_2L^{1-3}$(Tyr³-Oct) could be prepared on-resin or in-solution by treatment with $[tBu_4N][ReOCl_4]$ in methanol (Scheme 6). The on-resin approach is potentially of interest in producing radioactive complexes in high specific activity as unreacted $[ReO_4]^-$ and other impurities such as colloidal rhenium could be readily removed by filtration of the resin. The pure complex can be cleaved from the resin with 50% trifluoracetic acid and is stable to this relatively high concentration of acid. Analysis by HPLC and ESI-MS confirmed the identity of the complexes, with the $[ReO(HL^{1-3}(Tyr^3\text{-Oct}))_2]^+$ complexes showing signals in the ESI-MS that could be attributed to the 3+ molecular ion with expected rhenium isotope peak patterns (Figure 3).

**Preparation of $[^{188}Re(HL^1(Tyr^3\text{-Oct}))_2]^+$.** Preliminary radiolabeling of $H_2L^1$(Tyr³-Oct) with radioactive $^{188}Re$ was performed using generator-produced $[^{188}ReO_4]^-$. A solution of $[^{188}ReO_4]^-$, in an aqueous mixture of sodium chloride (0.9% w/v concentration) and sodium tartrate, was reduced with stannous chloride. This mixture was then reacted with $H_2L^1$(Tyr³-Oct) at 100 °C, leading to the formation of $[^{188}ReO(HL^1(Tyr^3\text{-Oct}))_2]^+$ in ca. 67% radiochemical yield. The compound was characterized by analytical reversed phased HPLC (Figure 4), where $[^{188}ReO(HL^1(Tyr^3\text{-Oct}))_2]^+$ (retention time = 11.6 min, detected using a NaI(Tl)) elutes with a similar retention time to the nonradioactive analogue $[^{nat}ReO(HL^1(Tyr^3\text{-Oct}))_2]^+$ (retention time = 11.3 min, detected at $\lambda_{220}$), where $^{nat}Re$ refers to naturally abundant Re isotopes. The small difference in retention times is due to the different configurations of the radioactivity and UV detectors. This elution profile of $[ReO(HL^1(Tyr^3\text{-Oct}))_2]^+$ is distinct from that of the free ligand, $H_2L^1$(Tyr³-Oct) that elutes at 9.7 min under the same conditions. Unreacted $^{188}Re$ species, presumably $[^{188}ReO_4]^-$, elute with the solvent front at 2.1 min (Figure 4).



DOI: 10.1021/acs.inorgchem.7b01247
Inorg. Chem. 2017, 56, 9725−9741

**Scheme 6. Reaction Scheme for the Formation of Octreotate-Derived Ligands $H_2L^{1-3}(Tyr^3\text{-Oct})$ and Corresponding Complexes, $[ReO(HL^{1-3}(Tyr_3\text{-Oct}))_2]^+$**

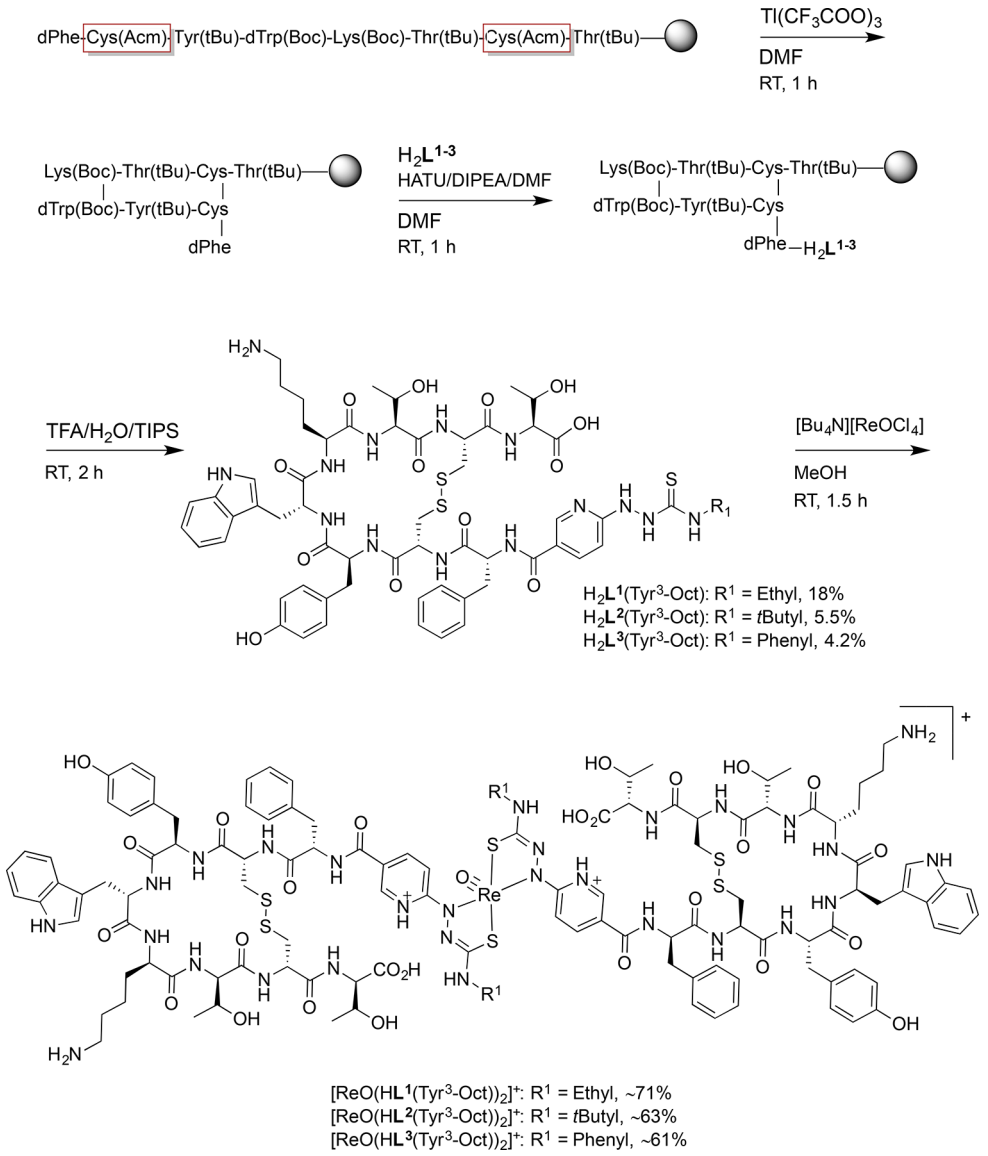


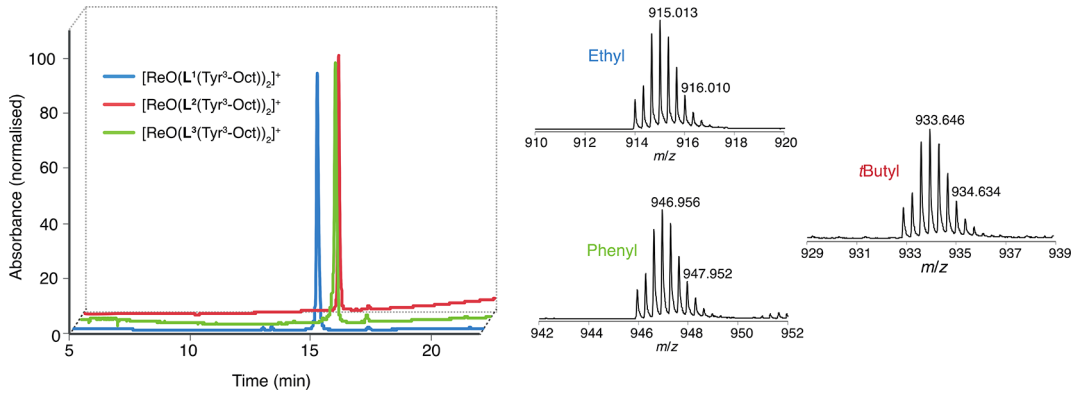


**Figure 3.** RP-HPLC chromatogram (UV absorbance, a.u., $\lambda$ 254 nm) of $Tyr^3$-octreotate rhenium complexes, $[ReO(HL^{1-3}(Tyr^3\text{-Oct}))_2]^+$. Inset: Positive ion ESI-MS data of major isotope peaks corresponding to each complex as the tripositive cation, $[ReO(HL^{1-3}(Tyr^3\text{-Oct}))_2]^{3+}$.

**Preparation of $^{99m}$Tc-Labeled Complexes, $[^{99m}TcO(HL^{1-3}(cRGDfK))_2]^+$ and $[^{99m}TcO(HL^{1-3}(Tyr^3\text{-Oct}))_2]^+$.** The technetium-99m complexes $[^{99m}TcO(HL^{1-3}(cRGDfK))_2]^+$ and $[^{99m}TcO(HL^{1-3}(Tyr^3\text{-Oct}))_2]^+$ were prepared in ca. 60−80% radiochemical yield using mild conditions and relatively simple procedures (Supporting Information, Figures S1 and S2).



DOI: 10.1021/acs.inorgchem.7b01247
Inorg. Chem. 2017, 56, 9725−9741

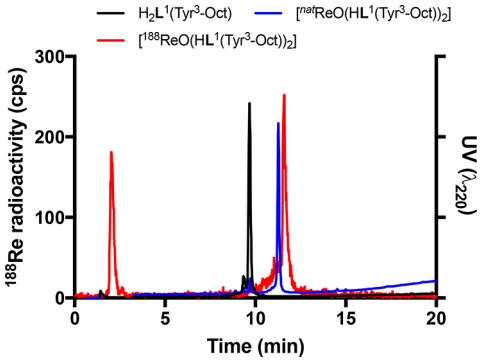


**Figure 4.** RP-HPLC chromatogram (UV absorbance, $\lambda$ 224 nm and radiation detection) of $[^{188/nat}ReO(HL^1(Tyr^3\text{-}Oct))_2]^+$ and free ligand $H_2L^1(Tyr^3\text{-}Oct)$. The signal at 2.1 min in the chromatogram of $[^{188}ReO(HL^1(Tyr^3\text{-}Oct))_2]^+$ corresponds to unreacted $^{188}Re$ species.

Preparation of $[^{99m}TcO(HL^{1-3}(cRGDfK))_2]^+$ and $[^{99m}TcO(HL^{1-3}(Tyr^3\text{-}Oct))_2]^+$ involved adding an excess of the appropriate ligand dissolved in aqueous sodium chloride (0.5 mg $mL^{-1}$, 0.9% NaCl, pH 7.4) to a mixture of $[^{99m}TcO_4]^-$ that has been reduced by tin(II) chloride in 0.1 M HCl in the presence of tartrate (pH 1−4) at room temperature. The radiolabeled $^{99m}Tc$ complexes were characterized by analysis by HPLC equipped with a radioactivity detector, and the elution profiles were compared to the analogous nonradioactive rhenium compounds (detected by UV absorbance). The close correlation between the retention times of the rhenium and technetium complexes strongly suggests that the complexes are isostructural (Table 3). The small difference in the retention times between the traces for $^{99m}Tc$ and Re complexes is, in part, due to the detector configurations but could also reflect the difference in polarity between the oxorhenium(V) and oxotechnetium(V) cores.

**Table 3. RP-HPLC Retention Times (min) for Ligands and $[MO(HL)_2]^+$ Complexes (M = Re, 99 mTc)·$L^1$ (ethyl), $L^2$ (*t*-butyl), and $L^3$ (phenyl) Compounds**[a]

| compound | $H_2L^x$ | rhenium complex | technetium complex |
|---|---|---|---|
| $L^1$-cRGDfK | 10.0 | 11.4 | 11.5 |
| $L^2$-cRGDfK | 9.3 | 10.3 | 10.9 |
| $L^3$-cRGDfK | 10.9 | 12.0 | 12.7 |
| $L^1$-($Tyr^3$-Oct) | 10.1 | 11.4 | 11.9 |
| $L^2$-($Tyr^3$-Oct) | 10.9 | 11.7 | 12.1 |
| $L^3$-($Tyr^3$-Oct) | 11.0 | 12.9 | 13.0 |

[a]Linear gradient from 0 to 90% Buffer B to A. Buffer A: 0.1% TFA in Milli-Q water. Buffer B: 0.1% TFA in $CH_3CN$.

The stability of $[^{99m}TcO(HL^3(Tyr^3\text{-}Oct))_2]^+$ was assessed by incubation in human plasma at 37 °C. The complex was stable for at least 2 h with only small amounts of degradation products (<5%) evident that, based on their retention times in analytical HPLC, are most likely due to degradation of the peptide.

## CONCLUDING REMARKS

The new pyridylthiocarbazide ligands (SHYNIC, $H_2L^{1-3}$) described here offer a useful alternative to the standard HYNIC system. While HYNIC has proved a very successful and versatile bifunctional ligand for $^{99m}Tc$ coligands are required to complete the coordination sphere of the metal ion and extrapolation to radioactive rhenium isotopes has been challenging.[3,63] This family of bidentate ligands form stable complexes with the $\{ReO\}^{3+}$ core with two ligands coordinated to a single metal ion. A rhenium complex with a methyl ester functional group has been characterized by X-ray crystallography and features the rhenium ion in a distorted square pyramidal environment with the oxo group in the apical position relative to the pseudo basal plane of two five-membered chelate rings with a *N,N/S,S trans* configuration about the Re-oxo core. The basic ligands have been decorated with the tumor targeting peptides cyclic-RGD and $Tyr^3$-octreotate, and these conjugates form complexes with rhenium to give well-defined single species, $[ReO((HL^{1-3})(cRGDfK))_2]$ and $[ReO((HL^{1-3})(Tyr^3\text{-octreotate}))_2]$, without having to add coligands resulting in the formation of a single structural and geometrical isomer. It is possible to form the rhenium complexes using either standard solution chemistry or "on-resin", and the latter approach may prove useful in isolating radioactive $^{188/186}Re$ analogues in high specific activity. These complexes feature two targeting peptides separated by 14 chemical bonds, and there is evidence that molecules containing more than one targeting peptide, sometimes referred to as bivalent, can display enhanced receptor binding due to simultaneous binding to more than one receptor on the surface on any given cell.[14,67−72] It is possible to prepare $[^{188}ReO(HL^1(Tyr^3\text{-}Oct))_2]^+$ in ∼67% yield from generator produced $[^{188}ReO_4]^-$, and improved yields should be possible by optimizing the reaction conditions. The analogous technetium complexes, $[TcO((HL^{1-3})(cRGDfK))_2]$ and $[TcO((HL^{1-3})(Tyr^3\text{-Octreotate}))_2]$, were prepared directly from $[^{99m}TcO_4]^-$ with tin chloride acting as a reducing agent. Comparison of HPLC profiles suggests the rhenium and technetium complexes are isostructural. The complexes described in this manuscript have two ligands coordinated to a single metal ion, whereas conventional HYNIC systems involve one HYNIC ligand binding to one metal ion. It is likely the two different systems will exhibit quite different biodistribution in vivo. These new systems warrant further investigation as potential theranostic agents employing an imaging ($^{99m}Tc$) and therapeutic ($^{186/188}Re$) matched pair for a single targeted agent.

**General Experimental.** All reagents were purchased from standard commercial sources. Nuclear magnetic resonance (NMR) spectra were acquired on either an Agilent 400-MR ($^1H$ NMR at 400 MHz and $^{13}C\{^1H\}$ NMR at 101 MHz) or a Varian FT-NMR 500 spectrometer ($^1H$ NMR at 500 MHz and $^{13}C\{^1H\}$ NMR at 126 MHz) at 298 K. Chemical shifts were referenced to residual solvent peaks and are quoted in ppm relative to TMS.

Fmoc-L-amino acids, Fmoc-D-amino acids, Nvoc-Cl, HATU, DIC, Wang resin, 2-chlorotrityl, Fmoc-Lys(ivDde)−OH, and Fmoc-Cys(Acm)−OH were purchased from standard commercial sources.

Linear protected RGDfK peptide (Arg(Pbf)-Gly(tBoc)-Asp(OtBu)-dPhe-Lys(tBoc)) was synthesized manually using standard Fmoc solid phase peptide synthesis (SPPS) procedures on the 2-chlorotrityl chloride resin. The linear pentapeptide was cleaved from the resin (with retention of protecting groups) using 1% TFA in dichloromethane and shaking for 40 min. The mixture was filtered and the filtrate was reduced in volume to afford crude linear product. Cyclization involved reacting the crude material in a mixture of dichloromethane (1 mg $mL^{-1}$), HATU (0.9 equiv), and DIPEA (6 equiv) at RT for 2 h, then evaporation to dryness


DOI: 10.1021/acs.inorgchem.7b01247
Inorg. Chem. 2017, 56, 9725−9741

*in vacuo*. A solution of TFA (97.5%) and Milli-Q water (2.5%) was added to the crude material to deprotect the peptide, followed by removal of the trifluoroacetic acid by sparging with a stream of $N_2$. The peptide was precipitated with diethyl ether, isolated by centrifugation (3 min, 3600 rpm) and dissolved in Milli-Q water (5 mL), and finally purified by semiprep RP-HPLC (Column 1); Gradient elution of Buffer A (0.1% TFA in $H_2O$) and Buffer B (0.1% TFA in $CH_3CN$) from 0 to 40% B to A, over 40 min (1.0% $min^{-1}$), UV detection at $\lambda$ 220 nm with a flow rate of 5 mL $min^{-1}$.

Linear protected $Tyr^3$-octreotate peptide, dPhe-Cys(Trt)-Tyr(tBu)-dTrp(tBoc)-Lys(tBoc)-Thr(tBu)-Cys(Trt)-Thr-(tBu)−OH,was synthesized using standard automated Fmoc SPPS procedures on a 2-chorotrityl chloride or Wang resin unless otherwise specified.[73]

Analytical reversed phase high performance liquid chromatography (RP-HPLC) was undertaken using an Agilent 1100 Series HPLC system at a flow rate of 1 mL $min^{-1}$ with either Column 1: A Zorbax Eclipse XDB-C18 column (150 mm × 4.6 mm, 5.0 $\mu$m) or Column 2: A Phenomenex Aeris Peptide XB-C18 column (250 mm × 4.6 mm, 3.6 $\mu$m). Solvent gradients for analytical analysis were either using System A: Gradient elution of Buffer A (0.1% TFA in $H_2O$) and Buffer B (0.1% TFA in $CH_3CN$) from 0 to 100% B over 25 min and UV detection at $\lambda$ 214, 254, and 280 nm, System B: Gradient elution of Buffer A (0.1% TFA in $H_2O$) and Buffer B (0.1% TFA in $CH_3CN$) from 0 to 60% B over 30 min and UV detection at $\lambda$ 214, 220, 254, 280, and 350 nm or System E: Gradient elution of Buffer A (0.1% TFA in $H_2O$) and Buffer B (0.1% TFA in $CH_3CN$) from 20 to 80% B, over 30 min and UV detection at $\lambda$ 220, 254, and 350 nm with a flow rate of 1 mL $min^{-1}$.

Semipreparative reversed phase high performance liquid chromatography (semiprep RP-HPLC) was performed using an Agilent 1200 series preparative HPLC unit with variable wavelength detector. An automated Agilent 1200 fraction collector collected 0.5−4 mL fractions. Peak separation was achieved using either Column 3: Kinetex C18 100 Å, AXIA column (150 mm × 21.2 mm, 5 $\mu$m), Column 4: Phenomenex Synergi Hydro-RP 80 Å (50 mm × 21.2 mm, 4 $\mu$m), Column 5: Varian Pursuit XRs C18 100 Å (150 × 21.2 mm, 5 $\mu$m) or Column 6: SGE ProteCol C18 120 Å (250 mm × 10 mm, 5 $\mu$m). Gradient elution, flow rate, and wavelength detection are compound specific and are detailed under the Experimental Section of a particular compound. Each fraction collected above 400 mAU was analyzed using ESI-MS and analytical HPLC.

Analytical HPLC traces of radiolabeled $^{188}Re$ compounds were acquired using an Agilent 1200 LC system with in-line UV and gamma detection (Flow-Count, LabLogic). Peak separation was achieved using an Agilent Eclipse XDB-C18 column (4.6 × 150 mm, 5 $\mu$m), with column 1 and system F: Gradient elution of Buffer A (0.1% TFA in $H_2O$) and Buffer B (0.1% TFA in $CH_3CN$) from 0 to 100% B over 20 min and UV detection at $\lambda$ 220 nm.

Analytical HPLC traces of radiolabeled $^{99m}Tc$ compounds were acquired using a Shimadzu 10 AVP UV−visible spectrophotometer (Shimadzu, Kyoto, Japan) and a sodium iodide scintillation detector with two LC-10ATVP solvent delivery systems for solvents A and B. Peak separation was achieved using Column 7: Nacalai Tesque Cosmosil 5C18-AR Waters column (4.6 × 150 mm, 5 $\mu$m) (Kyoto, Japan) at a flow rate of 1 mL $min^{-1}$. Gradient elution followed System C: Gradient elution of Buffer A (0.1% TFA in $H_2O$) and Buffer B (0.1% TFA in $CH_3CN$) from 0 to 100% B over 20 min and UV detection at $\lambda$ 254 nm.

X-ray structure determination and refinement was obtained for $[ReO(HL^1(OMe))_2]TFA$ on an Oxford Diffraction Super-Nova CCD diffractometer using Cu−K$\alpha$ radiation, and the temperature during data collection was maintained at 130.0(1) using an Oxford Cryosystems cooling device. The structure was solved by direct methods using SHELXT and refined using least-squares methods using SHELXL.[74,75] Thermal ellipsoid plots were generated using ORTEP-3 integrated within the WINGX suite of programs.[76] The trifluoroacetate counterion, although recognizable from the difference electron density maps, was badly disordered and could not be modeled satisfactorily. Application of the Squeeze procedure gave a void volume of 272 $Å^3$ containing 127 electrons, consistent with the presence of two trifluoroacetate anions per unit cell.[77] The charge on the complex is unambiguously (+1) given the presence of the two pyridinium protons which are involved in intramolecular hydrogen bonds and the ethylamino protons which are also involved in hydrogen bonds. The crystallographic data has been deposited in the Cambridge Structural Database (CCDC 1543360).

**Ligand Synthesis.** *Note: The designation of $H_2L^{1-4}$ refers to the structure with a carboxylic acid-substituted, pyridylhydrazine with the different thiocarbahydrazide functional groups (Et, tBu, and Ph respectively). Further derivatization of the carboxylate functional group is represented by placing the substituted group at the carboxylic carbon in replacement of the OH group (e.g., $H_2L^{1-3}(OMe)$, denotes the substitution of a methoxy at the carbonyl carbon to give a methyl ester.*

*6-[(2-Ethylcarbamothioyl)hydrazinyl]-3-pyridinecarboxylic acid, $H_2L^1$.* To a suspension of 6-hydrazino-3-pyridinecarboxylic acid[22] (0.45 g, 2.9 mmol) in anhydrous ethanol (5 mL) was added ethyl isothiocyanate (0.51 mL, 5.8 mmol) under an atmosphere of nitrogen. The suspension was heated to reflux for 16 h then cooled to RT, and the precipitate that formed was collected by filtration, washed with cold ethanol (20 mL), and diethyl ether (20 mL) to give $H_2L^1$ as a colorless powder (0.67 g, 95%). $^1H$ NMR [DMSO-$d_6$, 500 MHz]: $\delta$ (ppm) 9.39 (1H, s, N*H*), 9.01 (1H, s, N*H*), 8.63 (1H, d, $J$ = 1.7 Hz, py$H^2$), 8.19 (1H, t, $J$ = 4.8 Hz, N*H*), 8.04 (1H, dd, $J$ = 8.8, 2.2 Hz, py$H^4$), 6.53 (1H, d, $J$ = 8.8 Hz, py$H^5$), 3.45 (2H, dt, $J$ = 13.3, 6.8 Hz, $CH_2$), 1.03 (3H, t, $J$ = 7.1 Hz, $CH_3$); $^{13}C\{^1H\}$ NMR [DMSO-$d_6$, 125.7 MHz]: $\delta$ (ppm) 181.5 (C, NCS), 166.5 (C, $CO_2H$), 162.0 (C, py$C^6$), 150.4 (C, py$C^2$), 138.8 (C, py$C^4$), 117.8 (C, py$C^3$), 105.6 (C, py$C^5$), 38.4 (C, $CH_2$), 14.6 (C, $CH_3$); IR: $\overline{\nu}_{max}$ ($cm^{-1}$) 2981 (s/sh, N−H), 1605 (s/sh, C═O), 1539 (s/sh), 1319 (m/sh), 1282 (s/sh), 1245 (s/sh), 782 (s/sh); ESI-MS ($^+$): $m/z$ calc'd for $C_9H_{13}N_4O_2S$ 241.0759, found 241.0817 {[M + H]$^+$, 100%}; RP-HPLC (Column 1, System A): $R_T$ (min) 7.2.

*6-[2-(tert-Butylcarbamothioyl)hydrazinyl]-3-pyridinecarboxylic acid, $H_2L^2$.* To a suspension of 6-hydrazino-3-pyridinecarboxylic acid (0.45 g, 2.9 mmol) in anhydrous DMA (5 mL) was added *tert*-butyl isothiocyanate (0.56 mL, 4.4 mmol) under an atmosphere of nitrogen. The suspension was heated to 85 °C and after 30 min became a yellow mixture, which was heated at 85 °C for a further 3 h. The mixture was concentrated by evaporation under reduced pressure to a volume of approximately 1 mL and cold diethyl ether (15 mL) was added. The suspension was stirred vigorously overnight at RT. The precipitate was collected via filtration and washed with copious amounts of cold diethyl ether to afford an off-white


DOI: 10.1021/acs.inorgchem.7b01247
Inorg. Chem. 2017, 56, 9725−9741

solid (0.68 g, 86%). $^1$H NMR [MeOH-$d_4$, 500 MHz]: $\delta$ (ppm) 8.73 (1H, d, $J$ = 2.2 Hz, py$H^2$), 8.18 (1H, dd, $J$ = 8.7, 2.2 Hz, py$H^4$), 6.76 (1H, dd, $J$ = 8.7, 0.7 Hz, py$H^5$), 1.51 (9H, s); $^{13}$C{$^1$H} NMR [MeOH-$d_4$, 125.7 MHz]: $\delta$ (ppm) 181.0 (C, NCS), 166.1 (C, $CO_2$H), 162.0 (C, py$C^6$), 150.4 (C, py$C^2$), 138.8 (C, py$C^4$), 117.8 (C, py$C^3$), 105.6 (C, py$C^5$), 54.7 (C, -$C$(CH$_3$)$_3$), 29.0 (3C, -C($C$H$_3$)$_3$); IR: $\overline{\nu}_{max}$ (cm$^{-1}$) 1604 (s/sh, C═O), 1533 (s/sh), 1280 (s/sh), 1252 (s/sh), 1133 (m/sh), 1002 (m/sh), 779 (s/sh); HRMS (ESI$^+$): $m/z$ calc'd for $C_{11}H_{17}N_4O_2S$ 269.1072, found 269.1110 {[M + H]$^+$, 100%}; RP-HPLC (Column 1, System A): $R_T$ (min) 10.6.

*6-[2-(Phenylcarbamothioyl)hydrazinyl]-3-pyridinecarboxylic acid, $H_2$**L**$^3$.* To a suspension of 6-hydrazino-3-pyridinecarboxylic acid (0.45 g, 2.9 mmol) in anhydrous dimethylacetamide (DMA) (5 mL) was added phenyl isothiocyanate (0.59 mL, 4.4 mmol) under an atmosphere of nitrogen. The suspension was heated to 65 °C and after 5 min became a yellow solution, which was heated at 65 °C for a further 2 h. The mixture was concentrated by evaporation under reduced pressure to a volume of approximately 1 mL, and cold diethyl ether (15 mL) was added A precipitate was collected by filtration and washed with copious amounts of cold diethyl ether to afford an off-white powder (0.81 g, 97%). $^1$H NMR [DMSO-$d_6$, 400 MHz]: $\delta$ (ppm) 9.88 (1H, br s, N$H$), 9.84 (1H, br s, N$H$), 9.22 (1H, br s, N$H$), 8.67 (1H, d, $J$ = 1.9 Hz, py$H^2$), 8.07 (1H, d, $J$ = 8.4 Hz, py$H^4$), 7.47 (2H, d, $J$ = 7.2 Hz, Ar$H$), 7.30 (2H, t, $J$ = 7.2 Hz, Ar$H$), 7.13 (1H, t, $J$ = 7.2 Hz, Ar$H$), 6.66 (1H, d, $J$ = 8.8 Hz, py$H^5$); $^{13}$C{$^1$H} NMR [MeOH-$d_4$, 125.7 MHz]: $\delta$ (ppm) 181.3 (C, NCS), 166.4 (C, $CO_2$H), 161.7 (C, py$C^6$), 150.3 (C, py$C^2$), 139.2 (C, py$C^4$), 138.7 (C, Ar$C^1$), 127.9 (2C, Ar$C^{3,5}$), 125.6 (C, Ar$C^4$), 124.9 (2C, Ar$C^{2,6}$), 117.8 (C, py$C^3$), 106.1 (C, py$C^5$); IR: $\overline{\nu}_{max}$ (cm$^{-1}$) 1607 (s/sh, C═O), 1596 (s/sh), 1537 (s/sh), 1280 (s/sh), 1254 (s/sh), 1140 (m/sh), 1019 (m/sh), 782 (m/sh); HRMS (ESI$^+$): $m/z$ calc'd for $C_{13}H_{13}N_4O_2S$ 289.0759, found 289.0749 {[M + H]$^+$, 100%}; RP-HPLC (Column 1, System A): $R_T$ (min) 9.9.

*Methyl 6-Chloropyridine-3-carboxylate, **3**.* A suspension of 6-chloronicotinic acid (5.0 g, 32 mmol) in methanol (100 mL) was cooled to 0 °C, and $H_2SO_4$ (0.5 mL) was added dropwise. The mixture was heated at 60 °C for 8 h. The crude reaction mixture was evaporated to dryness under reduced pressure. The residue was dissolved in ethyl acetate and washed with sat. $NaHCO_3$. The organic layer was dried over $MgSO_4$, filtered, and evaporated to dryness in vacuo. The pale yellow solid was recrystallized from methanol to form clear, plate-like crystals (5.0 g, 91%). $^1$H NMR [$CHCl_3$-$d$, 400 MHz]: $\delta$ (ppm) 9.00 (1H, dd, $J$ = 2.4, 0.7 Hz, py$H^2$), 8.25 (1H, dd, $J$ = 8.3, 2.4 Hz, py$H^4$), 7.42 (1H, dd, $J$ = 8.3, 0.8 Hz, py$H^5$), 3.96 (3H, s, C$H_3$); $^{13}$C{$^1$H} NMR [$CHCl_3$-$d$, 125.7 MHz]: $\delta$ (ppm) 165.0 (C, $CO_2$Me), 155.8 (C, py$C^6$), 151.3 (C, py$C^2$), 139.8 (C, py$C^4$), 125.2 (C, py$C^3$), 124.4 (C, py$C^5$), 52.8 (C, OCH$_3$); ESI-MS ($^+$): $m/z$ calc'd for $C_7H_7ClNO_2$ 172.0165, found 171.9965 {[M + H]$^+$, 100%}; RP-HPLC (Column 2, System A): $R_T$ (min) 8.7.

*Methyl 6-Hydrazinyl-3-pyridinecarboxylate, **4**.* Methyl 6-chloropyridine-3-carboxylate, **3**, (0.10 g, 0.58 mmol), and hydrazine hydrate (50−60% $N_2H_4$, $d$ = 1.029 g cm$^{-3}$, 0.10 mL, approximately 3 equiv) were added to a 5 mL microwave vial, which was evacuated and purged with $N_2$. Degassed methanol (5 mL) was added to the vial, and the suspension was subjected to microwave irradiation for 15 min at 105 °C. The mixture was filtered and concentrated in vacuo. The residue obtained was dissolved in ethyl acetate and washed with sat. $NaHCO_3$ and sat. NaCl. The organic layer was collected and dried over $Na_2SO_4$, filtered, and concentrated to afford a chalky, yellow powder (0.08 g, 81%). $^1$H NMR [$CHCl_3$-$d$, 600 MHz]: $\delta$ (ppm) 8.95 (1H, d, $J$ = 2.4 Hz, py$H^2$), 8.21 (1H, dd, $J$ = 8.3, 2.4 Hz, py$H^4$), 7.40 (1H, d, $J$ = 8.3 Hz, py$H^5$), 3.92 (3H, s, OC$H_3$); $^{13}$C{$^1$H} NMR [$CHCl_3$-$d$, 151 MHz]: $\delta$ (ppm) 165.0 (C, $CO_2$Me), 155.7 (C, py$C^6$), 151.1 (C, py$C^2$), 139.7 (C, py$C^4$), 125.1 (C, py$C^3$), 124.3 (C, py$C^5$), 52.7 (C, OCH$_3$); HRMS (ESI$^+$): $m/z$ calc'd for $C_7H_{10}N_3O_2$ 168.0773, found 168.0777 {[M + H]$^+$, 100%}; RP-HPLC (Column 2, System A): $R_T$ (min) 7.6.

*Methyl 6-[(2-Ethylcarbamothioyl)hydrazinyl]-3-pyridinecarboxylate, $H_2$**L**$^1$(OMe).* Crude methyl 6-hydrazinyl-3-pyridinecarboxylate, **4**, (approximately 0.06 g, 0.67 mmol), was added to anhydrous ethanol (8 mL) and heated until entirely dissolved. Ethyl isothiocyanate (60 $\mu$L, 0.67 mmol) was added to the solution and stirred at reflux for 3 h. The solution was cooled to RT. A stream of $N_2$ was blown over the solution, and the resulting precipitate was collected by filtration and washed with copious amounts of diethyl ether to afford a colorless crystalline solid (0.05 g, 51%). $^1$H NMR [DMSO-$d_6$, 400 MHz]: $\delta$ (ppm) 9.41 (1H, s, -NHN$H$CS), 9.10 (1H, s, -N$H$NHCS), 8.66 (1H, d, $J$ = 1.8 Hz, py$H^2$), 8.21 (1H, br t, $J$ = 6.5 Hz, -N$H$CH$_2$CH$_3$), 8.06 (1H, dd, $J$ = 8.8, 2.1 Hz, py$H^4$), 6.55 (1H, d, $J$ = 8.8 Hz, py$H^5$), 3.80 (3H, s, OC$H_3$), 3.45 (2H, quin., $J$ = 6.6 Hz, C$H_2$CH$_3$), 1.03 (3H, t, $J$ = 7.1 Hz, CH$_2$C$H_3$); $^{13}$C{$^1$H} NMR [DMSO-$d_6$, 151 MHz]: $\delta$ (ppm) 181.3 (C, NCS), 165.4 (C, $CO_2$CH$_3$), 162.2 (C, py$C^6$), 150.2 (C, py$C^2$), 138.5 (C, py$C^4$), 116.7 (C, py$C^3$), 105.9 (C, py$C^5$), 51.9 (C, $CO_2$CH$_3$), 38.4 (C, $CH_2$), 14.6 (C, $CH_3$); IR: $\overline{\nu}_{max}$ (cm$^{-1}$) 3143 (m/br, N−H), 2977 (m/br), 1710 (s/sh, C═O), 1533 (m/br), 1295 (s/sh), 1254 (s/sh), 1240 (m/sh), 1119 (w/sh), 781 (m/sh); HRMS (ESI$^+$): $m/z$ calc'd for $C_{10}H_{15}N_4O_2$ 255.0916, found 255.0938 {[M + H]$^+$, 100%}; RP-HPLC (Column 2, System A): $R_T$ (min) 9.2.

*Methyl 6-[(2-tert-Butyllcarbamothioyl)hydrazinyl]-3-pyridinecarboxylate, $H_2$**L**$^2$(OMe).* The compound 6-[2-(*tert*-butylcarbamothioyl)hydrazinyl]-3-pyridinecarboxylic acid, ($H_2$**L**$^2$) (0.2 g, 0.74 mmol), was added to deoxygenated and dried $CH_3OH$ (20 mL). Sulfuric acid (~0.5 mL) was added dropwise, and the reaction was heated to 50−60 °C for 3 h. Addition of aqueous NaOH (0.1 M) caused a precipitate to form (pH 7−8). The precipitate was collected by filtration as a gray powder (0.13 g, 63%). $^1$H NMR [$CHCl_3$-$d$, 500 MHz]: $\delta$ (ppm) 8.74 (1H, d, $J$ = 1.7 Hz, py$H^2$), 8.16 (1H, dd, $J$ = 8.7, 2.2 Hz, py$H^4$), 6.76 (1H, dd, $J$ = 8.7, 0.3 Hz, py$H^5$), 3.86 (3H, s, $CO_2CH_3$), 1.47 (9H, s, ($CH_3$)$_3$); $^{13}$C{$^1$H} NMR [$CH_3OH$-$d_4$, 125.7 MHz]: $\delta$ (ppm) 180.9 (C, NCS), 165.6 (C, $CO_2CH_3$), 161.4 (C, py$C^6$), 150.6 (C, py$C^2$), 140.1 (C, py$C^4$), 119.8 (C, py$C^3$), 106.1 (C, py$C^5$), 53.8 (C, -OCH$_3$), 52.1 (C, -$C$(CH$_3$)$_3$), 28.7 (3C, -C($C$H$_3$)$_3$); IR: $\overline{\nu}_{max}$ (cm$^{-1}$) 1721 (s/sh, C═O), 1523 (m/sh), 1285 (s/sh), 1250 (s/sh), 1133 (m/sh), 775 (s/sh); ESI-MS ($^+$): $m/z$ calc'd for $C_{12}H_{19}N_4O_2S$ 283.1229, found 283.0450 {[M + H]$^+$, 100%}; RP-HPLC (Column 2, System A): $R_T$ (min) 12.9.

*Methyl 6-[(2-Phenylcarbamothioyl)hydrazinyl]-3-pyridinecarboxylate, $H_2$**L**$^3$(OMe).* The same procedure and reagents were used as for the synthesis of $H_2$L$^1$(OMe), except using phenyl isothiocyanate (45 $\mu$L, 0.38 mmol) and methyl 6-hydrazinyl-3-pyridinecarboxylate (63 mg, 0.38 mmol) to afford a white, microcrystalline solid (0.08 g, 71%). $^1$H NMR [$CH_3OH$-$d_4$, 400 MHz]: $\delta$ (ppm) 8.77 (1H, s, py$H^2$), 8.19 (1H, d, $J$ = 8.8 Hz, py$H^4$), 7.51 (2H, dd, $J$ = 8.1 Hz, Ar$H^{2,6}$),


DOI: 10.1021/acs.inorgchem.7b01247
Inorg. Chem. 2017, 56, 9725−9741

7.35 (2H, t, $J$ = 7.6 Hz, Ar$H^{3,5}$), 7.21 (1H, t, Ar$H^4$), 6.85 (1H, d, $J$ = 8.8 Hz, py$H^5$), 3.89 (3H, s, $CO_2CH_3$); $^{13}C\{^1H\}$ NMR [DMSO-$d_6$, 125.7 MHz]: $\delta$ (ppm) NCS resonance not detected, 165.0 (C, $CO_2$Me), 161.6 (C, py$C^6$), 150.4 (C, py$C^2$), 138.8 (C, Ar$C^1$), 137.7 (C, py$C^4$), 128.0 (2C, Ar$C^{3,5}$), 127.0 (C, Ar$C^4$), 124.6 (2C, Ar$C^{2,6}$), 116.6 (C, py$C^3$), 105.3 (C, py$C^5$), 51.8 (C, $CO_2CH_3$); IR: $\bar{\nu}_{max}$ ($cm^{-1}$) 3262 (m/sh, N−H), 1707 (s/sh, C═O), 1618 (m/sh), 1537 (s/sh), 1274 (s/sh), 1133 (m/sh), 742 (m/sh); ESI-MS ($^+$): $m/z$ calc'd for $C_{14}H_{15}N_4O_2S$ 303.0916, found 303.1274 {[M + H]$^+$, 100%}; RP-HPLC (Column 2, System A): $R_T$ (min) 13.1.

*$H_2L^1$(Lys).* Dichloromethane (10 mL) was added to 2-chlorotrityl resin (1.00 mmol $g^{-1}$ loading) (3.1 g, 3.1 mmol) swelling the resin. A mixture of $N_\alpha$-*t*Boc-$N_\varepsilon$-Fmoc-L-Lys (1.7 g, 3.6 mmol) and DIPEA (2.1 mL, 12 mmol) in dichloromethane (15 mL) was added to the resin, which was then shaken at ambient temperature for 2 h. The resin was filtered and the filtrate was discarded. The resulting resin was washed with dichloromethane (3 mL), DMF (3 mL), dichloromethane (3 mL), and finally diethyl ether (3 mL). After several hours of suction drying the resin was weighed and loading determined (0.77 mmol $g^{-1}$). To the dried resin-bound *t*Boc-Lys(Fmoc)−OH (0.51 g, 0.39 mmol) was added a DMF/piperidine (80:20 $v/v$) solution (20 mL), which was manually stirred. After 20 min, the supernatant was removed by filtration through a sintered frit, and the remaining resin was washed with DMF (3 mL). A positive TNBSA assay (2,4,6-trinitrobenzenesulfonic acid in methanol (5% $w/v$)) was used to indicate deprotection of the Fmoc protected epsilon ($\varepsilon$) amine. A mixture of HATU (285 mg, 0.75 mmol), $H_2\mathbf{L^1}$ (176 mg, 0.75 mmol), and DIPEA (261 $\mu$L, 1.5 mmol) in DMF (4 mL) was added to the resin and reacted for 4 h at ambient temperature. The liquid was drained and the resin was washed successively with dichloromethane (3 mL), then DMF (3 mL), and again with dichloromethane (3 mL). A TFA/$H_2O$/dichloromethane (18:2:80 $v/v$) solution was added to half the resin (approximately 0.19 mmol), and the mixture shaken for 1 h and then filtered. The filtrate was concentrated in vacuo and diethyl ether (40 mL) was added to form a suspension, which was centrifuged (3 min, 3600 rpm) and the supernatant was discarded. The crude material was dissolved in $H_2O/CH_3CN$ (90:10 $v/v$), filtered (Millipore 0.45 $\mu$m porosity syringe filter), and then purified by semipreparative RP-HPLC (Column 5). The HPLC system involved a gradient elution of Buffer A (0.1% TFA in $H_2O$) and Buffer B (0.1% TFA in $CH_3CN$) from 20 to 40% B to A, over 20 min (1.0% $min^{-1}$) then 40−60% over 40 min (0.5% $min^{-1}$) and UV detection at 220 nm with a flow rate of 5 mL $min^{-1}$. Fractions containing the desired compound were identified by HPLC-MS, consolidated and lyophilized to afford an off-white, fluffy compound (10 mg, 14%). ESI-MS ($^+$): $m/z$ calc'd for $C_{15}H_{25}N_6O_3S$ 369.1709, found 369.1798 {[M + H]$^+$, 100%}; RP-HPLC (Column 2, System A): $R_T$ (min) 6.00, (Column 2, System B) 24.0.

*$H_2L^2$($N_\alpha$OAc-Lys-OMe).* A solution of HATU (0.23 g, 0.56 mmol) and DIPEA (0.29 mL, 1.1 mmol) in DMSO (1 mL) was added to $H_2\mathbf{L^2}$ (0.15 g, 0.56 mmol) and shaken for 2 min. $N_\alpha$-Acetyl-L-lysine methyl ester hydrochloride (0.10 g, 0.42 mmol) in DMSO (1 mL) was added and shaken for 2 h. Diethyl ether (40 mL) was added and the mixture was centrifuged. The supernatant was discarded and the remaining yellow oil was purified by semipreparative RP-HPLC (Column 5). The HPLC system involved a gradient elution of Buffer A (0.1% TFA in $H_2O$) and Buffer B (0.1% TFA in $CH_3CN$) from 10 to 60% B to A, over 50 min (1.0% $min^{-1}$) and UV detection at $\lambda$ 220 and 254 nm with a flow rate of 5 mL $min^{-1}$. Fractions containing the desired compound were identified by HPLC-MS, consolidated, and lyophilized to afford a colorless fluffy solid (0.19 g, 27%). $^1$H NMR [MeOH-$d_4$, 600 MHz]: $\delta$ (ppm) 8.48 (1H, d, $J$ = 2.1 Hz, py$H^2$), 8.29 (1H, dd, $J$ = 9.1, 2.2 Hz, py$H^4$), 7.05 (1H, d, $J$ = 9.1 Hz, py$H^5$), 4.38 (1H, dd, $J$ = 8.9, 5.2 Hz, $\alpha CH$), 3.70 (3H, s, $CO_2CH_3$), 3.38 (2H, t, $J$ = 7.2 Hz, $\varepsilon CH_2$), 1.97 (3H, s, $COCH_3$), 1.87−1.84 (1H, m, $\beta CH_2$), 1.75−1.69 (1H, m, $\beta CH_2$), 1.65−1.61 (2H, m, $\delta CH_2$), 1.53 (9H, s, $(CH_3)_3$), 1.49−1.41 (2H, m, $\gamma CH_2$); $^{13}C\{^1H\}$ NMR [MeOH-$d_4$, 150.9 MHz]: $\delta$ (ppm) 184.0 (C, NCS), 174.2 (C, -$COCH_3$), 173.4 (C, -$CO_2CH_3$), 165.9 (C, CONH), 159.1 (C, py$C^6$), 149.4 (C, py$C^2$), 141.4 (C, py$C^4$), 123.7 (C, py$C^3$), 110.6 (C, py$C^5$), 54.9 (C, -$C(CH_3)_3$), 53.7 (C, $\alpha CH_2$), 52.7 (C, $-CO_2CH_3$), 40.7 (C, $\varepsilon CH_2$), 32.1 (C, $\beta CH_2$), 29.8 (C, $\delta CH_2$), 28.9 (3C, -$C(CH_3)_3$), 24.2 (C, $-COCH_3$), 22.3 (C, $\gamma CH_2$); HRMS (ESI$^+$): $m/z$ calc'd for $C_{20}H_{33}N_6O_4S$ 453.2284, found 453.2288 {[M + H]$^+$, 100%}; RP-HPLC (Column 2, System A): $R_T$ (min) 12.5.

*$H_2L^1$(cRGDfK).* To a solution of 6-[(2-ethylcarbamothioyl)-hydrazinyl]-3-pyridinecarboxylic acid, ($H_2\mathbf{L^1}$) (16 mg, 66 $\mu$mol) in DMF (0.5 mL) was added HATU (25 mg, 66 $\mu$mol) and DIPEA (23 $\mu$L, 0.13 mmol). A solution of cRGDfK (10 mg, 17 $\mu$mol) in DMF (0.3 mL) was added to the initial mixture and then shaken for 2 h at ambient temperature. Diethyl ether (40 mL) was added and the subsequent suspension centrifuged (3 min, 3600 rpm). The supernatant was discarded and the process repeated. The remaining solid was dissolved in a $H_2O/CH_3CN$ (90:10 $v/v$) solution, filtered (Millipore 0.45 $\mu$m porosity syringe filter), and then purified by semipreparative RP-HPLC (Column 4). The HPLC system involved a gradient elution of Buffer A (0.1% TFA in $H_2O$) and Buffer B (0.1% TFA in $CH_3CN$) from 0 to 50% B to A, over 65 min (1.3% $min^{-1}$) and UV detection at $\lambda$ 220, 254, 275, and 350 nm with a flow rate of 8 mL $min^{-1}$. Fractions containing the desired compound were identified by HPLC-MS, consolidated and lyophilized to afford a colorless solid (10 mg, 80%). ESI-MS ($^+$) $m/z$ calc'd for $[C_{36}H_{52}N_{13}O_8S]^+$ 826.378, found 826.376, calc'd for $[C_{36}H_{53}N_{13}O_8S]^{2+}$ 413.693, found 413.692; RP-HPLC (Column 2, System A): $R_T$ (min) 11.3.

*$H_2L^2$(cRGDfK).* The same procedure was used as for $H_2\mathbf{L^1}$(cRGDfK), except $H_2\mathbf{L^1}$ was replaced with 6-[(2-*tert*-butylcarbamothioyl)hydrazinyl]-3-pyridinecarboxylic acid, ($H_2\mathbf{L^2}$) (5.3 mg, 19 $\mu$mol), and other reagent quantities were adapted accordingly; HATU (6.5 mg, 17 $\mu$mol), DIPEA (45 $\mu$L, 0.13 mmol), and cRGDfK (10 mg, 17 $\mu$mol). Semi-preparative RP-HPLC purification (Column 4) involved a gradient elution of Buffer A (0.1% TFA in $H_2O$) and Buffer B (0.1% TFA in $CH_3CN$) from 0 to 40% B to A, over 80 min (0.5% $min^{-1}$) and UV detection at $\lambda$ 220, 254, 275, and 350 nm with a flow rate of 8 mL $min^{-1}$. Fractions containing the desired compound were identified by HPLC-MS, consolidated and lyophilized to afford a light yellow solid (3.4 mg, 24%). ESI-MS ($^+$) $m/z$ calc'd for $[C_{38}H_{56}N_{13}O_8S]^+$ 854.4096, found 854.4097, calc'd for $[C_{38}H_{57}N_{13}O_8S]^{2+}$ 427.7087, found 427.7083; RP-HPLC (Column 2, System A): $R_T$ (min) 12.9.

*$H_2L^3$(cRGDfK).* The same procedure was used as for $H_2\mathbf{L^1}$(cRGDfK), except $H_2\mathbf{L^1}$ was replaced with 6-[(2-phenylcarbamothioyl)hydrazinyl]-3-pyridinecarboxylic acid, ($H_2\mathbf{L^3}$) (5.2 mg, 19 $\mu$mol) and other reagent quantities were adapted accordingly; HATU (6.8 mg, 18 $\mu$mol), DIPEA (45



DOI: 10.1021/acs.inorgchem.7b01247
*Inorg. Chem.* 2017, 56, 9725−9741

μL, 0.13 mmol), and cRGDfK (10 mg, 17 μmol). Semi-preparative RP-HPLC purification (Column 4) involved a gradient elution of Buffer A (0.1% TFA in $H_2O$) and Buffer B (0.1% TFA in $CH_3CN$) from 0 to 40% B to A, over 80 min (0.5% $min^{-1}$) and UV detection at λ 214, 220, and 254 nm with a flow rate of 8 mL $min^{-1}$. Fractions containing the desired compound were identified by HPLC-MS, consolidated, and lyophilized to afford a colorless solid (8.6 mg, 55%). ESI-MS (+) *m/z* calc'd for $[C_{40}H_{52}N_{13}O_8S]^+$ 874.3783, found 874.3380, calc'd for $[C_{40}H_{53}N_{13}O_8S]^{2+}$ 437.6930, found 437.6992; RP-HPLC (Column 2, System A): $R_T$ (min) 14.2.

*$H_2L^1$(Tyr³-Oct).* Linear protected Tyr³-octreotate peptide (dPhe-Cys(Acm)-Tyr(*t*Bu)-dTrp(*t*Boc)-Lys(*t*Boc)-Thr(*t*Bu)-Cys(Acm)-Thr(*t*Bu)-OH) was prepared manually by standard Fmoc SPPS on Wang resin preloaded with H-Thr(*t*Bu)−OH (100 mg, 0.5 mmol $g^{-1}$). Amino acid coupling: Coupling of each amino acid was achieved by addition to the resin of a premade solution of Fmoc-amino acid (2 mmol, 4 equiv), HATU (1.9 mmol, 3.8 equiv), and DIPEA (4 mmol, 8 equiv) in DMF (5 mL). The resin mixture was shaken in a reaction vessel equipped with a sintered bottom for 1 h then filtered and washed with DMF (3 mL), dichloromethane (3 mL), and again with DMF (3 mL). Successful coupling was confirmed by a negative TNBSA test. Fmoc deprotection: Cleavage of the Fmoc groups was achieved after each successive coupling reaction. A DMF/piperidine (80:20 *v/v*) solution was added to the protected resin, which was contained in a reaction vessel with a sintered frit. The mixture was stirred for 5 min, and then the resin was filtered and washed with cleavage solution, then DMF (2 mL), dichloromethane (2 mL) and again DMF (3 mL). Complete deprotection was confirmed with a positive TNBSA test. Acm-group deprotection and on-resin cyclization: After the final Fmoc deprotection of resin-bound Fmoc-dPhe-OH, thallium(III) trifluoroacetate ($Tl(CF_3CO_2)_3$) (0.54 g, 1.0 mmol, 2 equiv) in DMF (4 mL) was added to the resin, and the mixture was stirred for 2 h. The liquid was decanted from the resin and the resin was washed with DMF (15 mL), dichloromethane (3 mL), and diethyl ether (2 mL). SHYNIC coupling: Half the resin-bound peptide (approximately 0.25 mmol) was used for the following reaction. $H_2L^1$ (0.18 g, 0.75 mmol, 3 equiv) was dissolved in DMF (3 mL) and HATU (0.29 g, 0.75 mmol, 3 equiv) added to preactivate the ligand. DIPEA (0.26 mL, 1.5 mmol, 6 equiv) was added and the mixture shaken for 2 min until full dissolution had occurred. The yellow solution was added to the dry resin in a reaction vessel equipped with a sintered frit and shaken for 2 h. The reaction solution was drained and the resin was washed with DMF (15 mL), dichloromethane (3 mL) and again DMF (3 mL). Resin and acid-sensitive protecting group cleavage: The petide-loaded resin was treated with a TFA/TIPS/$H_2O$ (96:1.5:2.5 *v/v/v*) solution (20 mL) and shaken for 2 h. The mixture was filtered and sparged with a steady stream of $N_2$ to reduce the volume by 90%. Cold diethyl ether (40 mL) was added to precipitate the peptide that was isolated by centrifugation (3 min, 3600 rpm). The crude material was dissolved in $CH_3CN/H_2O$ (50:50 *v/v*) and lyophilized. The solid was dissolved in $CH_3CN/H_2O$ (40:60 *v/v*) and filtered (Millipore 0.45 μm porosity syringe filter). The compound was purified by semipreparative RP-HPLC (Column 5) with a linear gradient elution of Buffer A (0.1% TFA in $H_2O$) and Buffer B (0.1% TFA in $CH_3CN$) from 20 to 80% B to A, over 120 min (0.5% $min^{-1}$) and UV detection at λ 214, 220, 254, 280, and 350 nm with a flow rate of 8 mL $min^{-1}$. Fractions containing the desired compound were identified by HPLC-MS, consolidated and lyophilized to afford a pale yellow solid (56 mg, 18%). HRMS (+) *m/z* calc'd for $[C_{58}H_{75}N_{14}O_{13}S_3]^+$ 1271.4800, found 1271.4760, calc'd for $[C_{58}H_{75}N_{14}O_{13}S_3]^{2+}$ 636.2439, found 636.2416; RP-HPLC (Column 2, System A): $R_T$ (min) 13.0.

*$H_2L^2$(Tyr³-Oct).* The same procedure was used as for $H_2L^1$(Tyr³-Oct), except $H_2L^1$ was replaced with $H_2L^2$ (0.20 g, 0.75 mmol, 3 equiv), and all other reagents were used according to their reported equivalencies. The precipitate after lyophilization was dissolved in $CH_3CN/H_2O$ (8 mL, 50:50 *v/v*) and filtered (Millipore 0.45 μm porosity syringe filter). The compound was purified by semipreparative RP-HPLC (Column 5) with an isocratic step gradient system of Buffer A (0.1% TFA in $H_2O$) and Buffer B (0.1% TFA in $CH_3CN$). The elution method involved 28% B for 10 min then 32% B for 40 min (desired peak at 34 min) and UV detection at λ 214, 220, 254, 280, and 350 nm with a flow rate of 8 mL $min^{-1}$. Fractions containing the desired compound were identified by HPLC-MS, consolidated, and lyophilized to afford a fluffy, colorless compound (18 mg, 5.5%). HRMS (+) *m/z* calc'd for $[C_{60}H_{79}N_{14}O_{13}S_3]^+$ 1299.5113, found 1299.5110, calc'd for $[C_{60}H_{80}N_{14}O_{13}S_3]^{2+}$ 650.2596, found 650.2599; RP-HPLC (Column 2, System A): $R_T$ (min) 14.4.

*$H_2L^3$(Tyr³-Oct).* The same procedure was used as for $H_2L^1$(Tyr³-Oct), except $H_2L^1$ was replaced with $H_2L^3$ (0.22 g, 0.75 mmol, 3 equiv). The precipitate after lyophilization was dissolved in $CH_3CN/H_2O$ (10 mL, 50:50 *v/v*) and filtered (Millipore 0.45 μm porosity syringe filter). The compound was purified by semipreparative RP-HPLC (Column 5) with a linear gradient system of Buffer A (0.1% TFA in $H_2O$) and Buffer B (0.1% TFA in $CH_3CN$) from 20% to 50% B to A over 60 min (0.5% $min^{-1}$) (or isocratic elution at 29% Buffer B) and UV detection at λ 254 nm with a flow rate of 7 mL $min^{-1}$. Fractions containing the desired compound were identified by HPLC-MS, consolidated and lyophilized to afford a fluffy white solid (14 mg, 4.2%). HRMS (+) *m/z* calc'd for $[C_{62}H_{75}N_{14}O_{13}S_3]^+$ 1319.4800, found 1319.4849, calc'd for $[C_{62}H_{75}N_{14}O_{13}S_3]^{2+}$ 650.2596, found 636.2425; RP-HPLC (Column 2, System A): $R_T$ (min) 14.1.

**Synthesis of Rhenium Complexes.** *Note: Unless specified Re represents 'rhenium with natural isotope abundance'.*

*[ReO(HL¹(OMe))₂]Cl.* To $H_2L^1$(OMe) (90 mg, 0.35 mmol) and ($tBu_4N$)[$ReOCl_4$] (103 mg, 0.18 mmol) was added anhydrous MeOH (13 mL). The mixture immediately turned deep red and was stirred at room temperature for 4 h. The reaction mixture was filtered, diethyl ether (ca. 15 mL) was added, and the resulting precipitate was collected by filtration to give $[ReO(HL^1(OMe))_2]Cl$ as a dark-red, microcrystalline solid (0.11 g, 84%). $^1H$ NMR [DMSO-$d_6$, 400 MHz]: δ (ppm) 8.63 (2H, s, py$H^2$), 8.26 (2H, dd, *J* = 9.3, 1.8 Hz, py$H^5$), 7.87 (2H, d, *J* = 9.4 Hz, py$H^4$), 7.43 (2H, br m, N*H*), 3.89 (6H, s, OC$H_3$), 3.47 (4H, qd, *J* = 13.6, 7.0 Hz, C$H_2$CH$_3$), 1.16 (6H, t, *J* = 7.5 Hz, CH$_2$C$H_3$); $^{13}C\{^1H\}$ NMR [$CH_3CN$-$d_3$, 150.9 MHz]: δ (ppm) 173.7 (2C, $CO_2CH_3$), 165.1 (2C, N═CS), 162.5 (2C, py$C^6$), 140.5 (2C, py$C^5$), 139.9 (2C, py$C^2$), 123.9 (2C, py$C^4$), 122.0 (2C, py$C^3$), 52.3 (2C, $CO_2CH_3$), 42.6 (2C, $CH_2CH_3$), 14.5 (2C, $CH_2CH_3$); IR: $\bar{\nu}_{max}$ ($cm^{-1}$) 1553 (s/sh, C═O), 1287 (s/sh), 963 (m/sh, Re═O), 764 (m/sh); HRMS ($ESI^+$): *m/z* calc'd for $ReC_{20}H_{26}N_8O_5S_2$ 709.0916, found 709.0898 {[M]$^+$, 100%}; RP-HPLC (Column 2, System A): $R_T$ (min) 14.8.

*Histidine and Cysteine Challenge Experiments.* A 50-fold excess of histidine or cysteine was added to a solution of



DOI: 10.1021/acs.inorgchem.7b01247
*Inorg. Chem.* 2017, 56, 9725−9741

$[ReO(HL^1(OMe))_2]^+$ (1 mg/L) in PBS Buffer (10 mM, pH 7.4, 4 mL) and the mixture was heated to 37 °C. At 2, 4, and 24 h after initiation of the experiment, 10 μL aliquots of the reaction mixture were diluted with 90 μL of Milli-Q water and analyzed using analytical HPLC methods. The HPLC traces showed little or no decomposition (<5%) of the rhenium complex at all the time-points.

*[ReO(HL²(OMe))₂]BPh₄.* To a stirred suspension of *trans*-$[ReOCl_3(PPh_3)_2]$ (0.15 g, 0.17 mmol) in MeOH (10 mL) was added $H_2L^2(OMe)$ (0.10 g, 0.35 mmol) and 2 drops of $Et_3N$. The mixture was heated at reflux for 16 h, then filtered, and diethyl ether was added to the filtrate. The resulting precipitate was collected by filtration, washed with cold diethyl ether, and then dissolved in MeOH. Addition of excess $NaBPh_4$ resulted in the precipitation of a red-brown precipitate that was collected, and washed with hot hexane (10 mL) to afford $[ReO(HL^2(OMe))_2]BPh_4$ (72 mg, 39%). $^1H$ NMR [$CHCl_3$-*d*, 600 MHz]: δ (ppm) 8.10 (2H, d, *J* = 9.5 Hz, py*H*²), 7.75 (2H, d, *J* = 9.4 Hz, py*H*⁵), 7.62 (8H, m, BAr*H*), 7.33 (2H, m, py*H*⁴), 6.93 (8H, t, *J* = 7.1 Hz, BAr*H*), 6.72 (4H, t, *J* = 7.1 Hz, BAr*H*), 3.86 (6H, s, $CO_2CH_3$), 1.39 (18H, s, $(CH_3)_3$); $^{13}C\{^1H\}$ NMR [$CHCl_3$-*d*, 150.9 MHz]: δ (ppm) 164.5, 142.5, 135.8−135.8 (8C, BAr*C*), 133.9−133.8, 128.9, 128.6, 128.5, 127.5, 126.2−126.1 (8C, BAr*C*), 122.0 (4C, BAr*C*), 54.9 (2C, -O*C*H₃), 52.6 (2C, -*C*(CH₃)₃), 29.0 (6C, -C(*C*H₃)₃); IR: $\bar{\nu}_{max}$ ($cm^{-1}$) 1555 (s/sh, C═O), 1284 (s/sh), 960 (m/sh, Re═O), 756 (m/sh); HRMS ($ESI^+$): *m*/*z* calc'd for $ReC_{24}H_{34}N_8O_5S_2$ 765.1651, found 765.1559 {$[M]^+$, 100%}; RP-HPLC (Column 2, System A): $R_T$ (min) 15.0.

*[ReO(HL³(OMe))₂]Cl.* The same procedure was used as for $[ReO(HL^1(OMe))_2]^+$, except $H_2L^1(OMe)$ was replaced with $H_2L^3(OMe)$ (0.10 g, 0.33 mmol). All other reagents quantities were used accordingly; $(tBu_4N)[ReOCl_4]$ (95 mg, 0.16 mmol) and MeOH (20 mL). The reaction afforded a red microcrystalline solid (69 mg, 51%). $^1H$ NMR [DMSO-$d_6$, 400 MHz]: δ (ppm) 9.84 (2H, s, N*H*), 8.79 (2H, s, py*H*²), 8.42 (2H, dd, *J* = 9.1, 1.7 Hz, py*H*⁵), 8.03 (2H, d, *J* = 9.2 Hz, py*H*⁴), 7.73 (4H, d, *J* = 7.8 Hz, Ar*H*²,⁶), 7.32 (4H, t, *J* = 7.9 Hz, Ar*H*³,⁵), 6.95 (2H, t, *J* = 7.3 Hz, Ar*H*⁴), 3.92 (6H, s, $CO_2CH_3$); $^{13}C\{^1H\}$ NMR [DMSO-$d_6$, 150.9 MHz]: δ (ppm) $CO_2Me$ signal not detected, 164.2 (2C), 145.5 (2C), 142.2 (2C, py*C*⁵), 139.5 (2C, py*C*²), 130.0 (2C, Ar*C*³,⁵), 129.3 (4C, Ar*C*⁴), 128.9 (2C, Ar*C*¹), 122.3 (2C, py*C*⁴), 121.4 (2C, py*C*³), 117.6 (4C, Ar*C*²,⁶), 52.6 (2C, $CO_2CH_3$)₃); IR: $\bar{\nu}_{max}$ ($cm^{-1}$) 1557 (s/sh, C═O), 1282 (s/sh), 960 (m/sh, Re═O), 752 (m/sh); HRMS ($ESI^+$): *m*/*z* calc'd for $ReC_{28}H_{26}N_8O_5S_2$, 805.1014, found 805.1004 {$[M]^+$, 100%}; RP-HPLC (Column 2, System A): $R_T$ (min) 15.4.

*[ReO(HL²(Nα-Ac-Lys-OMe))₂]⁺.* To $H_2L^2(N_\alpha$-Ac-Lys-OMe) (15 mg, 33 μmol) in MeOH (1 mL) was added a solution of $(tBu_4N)[ReOCl_4]$ (0.9 mg, 15 μmol) in MeOH (0.3 mL). The mixture was stirred at ambient temperature for 2 h, then diluted with Milli-Q water and purified by semipreparative RP-HPLC (Column 4). The HPLC system involved a gradient elution of Buffer A (0.1% TFA in $H_2O$) and Buffer B (0.1% TFA in $CH_3CN$) from 10 to 20% B to A, over 10 min (1.0% $min^{-1}$), then 20 to 40% B to A over 40 min (0.5% $min^{-1}$) and UV detection at λ 214, 220, 254, and 280 nm with a flow rate of 8 mL $min^{-1}$. Fractions containing the desired compound were identified by HPLC-MS, consolidated and lyophilized to afford a red solid (5 mg, 27%, assuming $[ReO(HL^2(N_\alpha$-Ac-Lys-OMe))$_2]CF_3CO_2$). $^1H$ NMR [MeOH-$d_4$, 600 MHz]: δ (ppm) 8.68 (2H, s, py*H*²), 8.36 (2H, d, *J* = 9.6 Hz, py*H*⁵), 8.03 (2H, d, *J* = 9.5 Hz, py*H*⁴), 4.43−4.40 (2H, m, α*CH*), 3.72 (6H, s, $CO_2CH_3$), 3.43 (4H, q, *J* = 6.6 Hz, ε$CH_2$), 1.99 (6H, s, $COCH_3$), 1.92−1.86 (4H, m, β$CH_2$), 1.78−1.72 (4H, m, δ$CH_2$), 1.71−1.66 (4H, m, γ$CH_2$), 1.50 (18H, s, $(CH_3)_3$); $^{13}C\{^1H\}$ NMR [MeOH-$d_4$, 150.9 MHz]: δ (ppm) 174.2 (2C, $COCH_3$), 173.4 (2C, $CO_2CH_3$), 167.2 (2C, N = *C*S), 165.1 (2C, *C*ONH), 163.3 (2C, py*C*⁶), 140.7 (2C, d, py*C*⁵), 139.1 (2C, d, py*C*²), 124.5 (2C, py*C*⁴), 122.6 (2C, py*C*³), 55.3 (2C, -*C*(CH₃)₃), 53.7 (C, α$CH_2$), 52.7 (C, −$CO_2CH_3$), 40.8 (2C, ε$CH_2$), 32.1 (2C, β$CH_2$), 29.9 (2C, δ$CH_2$), 28.9 (6C, -C(*C*H₃)₃), 24.3 (2C, $COCH_3$), 22.3 (2C, γ$CH_2$); HRMS ($ESI^+$) *m*/*z* calc'd for $[ReC_{40}H_{62}N_{12}O_9S_2]^+$ 1105.3762, found 1105.4079, calc'd for $[ReC_{40}H_{62}N_{12}O_9S]^{2+}$ 553.1920, found 553.2094; RP-HPLC (Column 2, System A): $R_T$ (min) 16.9.

*[ReO(HL¹(Lys))₂]⁺.* To resin-bound $H_2L^1$(Lys) (approximately 0.19 mmol) was added *trans*-$[ReOCl_3(PPh_3)_2]$ (78 mg, 0.09 mmol) suspended in DMF (5 mL). The slurry was stirred for 2 h. The green suspension turned colorless and the resin turned dark red. The red resin was isolated by filtration and washed with DMF (3 mL), dichloromethane (3 mL), and again with DMF (3 mL). The rhenium complex was cleaved from the resin by treatment with TFA/dichloromethane (50:50 *v*/*v*) solution (30 mL) for 3 h. The mixture was sparged with $N_2$ to reduce the volume to 10% of the original volume. Cold diethyl ether (40 mL) was added, the mixture was centrifuged (3 min, 3600 rpm), and the supernatant was discarded. This process was repeated twice. The precipitate was dissolved in $CH_3CN$ (1.0 mL) and then Milli-Q water (2.0 mL) was added. The complex was purified by semipreparative RP-HPLC purification (Column 5) involved a gradient elution of Buffer A (0.1% TFA in $H_2O$) and Buffer B (0.1% TFA in $CH_3CN$) from 10 to 70% B to A, over 120 min (0.5% $min^{-1}$) and UV detection at λ 214, 220, and 254 nm, with a flow rate of 8 mL $min^{-1}$. Fractions containing the desired compound were identified by HPLC-MS, consolidated, and lyophilized to afford a red, fluffy solid (22 mg, 23%, assuming $[ReO(HL^1(Lys))_2]$-$CF_3CO_2$). $^1H$ NMR [MeOH-$d_4$, 600 MHz]: δ (ppm) 8.58 (2H, s, py*H*²), 8.34 (2H, dd, *J* = 9.5, 1.8 Hz, py*H*⁵), 7.97 (2H, d, *J* = 9.5 Hz, py*H*⁴), 3.80 (2H, t, *J* = 6.1 Hz, α*CH*), 3.60 (4H, dtd, *J* = 20.2, 13.2, 7.0 Hz, −$CH_2CH_3$), 3.46 (4H, dd, *J* = 8.9, 5.1 Hz, ε$CH_2$), 1.99−1.92 (4H, m, β$CH_2$), 1.72 (4H, dt, *J* = 14.5, 7.3 Hz, δ$CH_2$), 1.60−1.50 (4H, m, γ$CH_2$), 1.27 (6H, t, −$CH_2CH_3$); $^{13}C\{^1H\}$ NMR [MeOH-$d_4$, 150.9 MHz]: δ (ppm) 172.8 (2C, $CO_2H$), 169.0 (2C, N═*C*S), 165.4 (2C, *C*ONH), 163.6 (2C, py*C*⁶), 140.5 (2C, py*C*⁵), 138.9 (2C, py*C*²), 123.9 (2C, py*C*⁴), 122.5 (2C, py*C*³), 54.9 (2C, α*C*H), 42.5 (2C, $CH_2CH_3$), 40.6 (2C, ε$CH_2$), 31.5 (2C, β$CH_2$), 29.9 (2C, δ$CH_2$), 23.4 (2C, γ$CH_2$), 14.9 (2C, $CH_2CH_3$); ESI-MS (⁺) *m*/*z* calc'd for $[ReC_{30}H_{46}N_{12}O_7S_2]^+$ 937.2611, found 937.2574, calc'd for $[ReC_{30}H_{47}N_{12}O_7S_2]^{2+}$ 469.1345, found 469.1355, calc'd for $[ReC_{30}H_{48}N_{12}O_7S_2]^{3+}$ 313.0256, found 313.0939; RP-HPLC (Column 2, System A): $R_T$ (min) 10.1.

*[ReO(HL¹(cRGDfK))₂]⁺.* A solution of $H_2L^1$(cRGDfK) (5 mg, 6.1 μmol) in MeOH (250 μL) was added to a mixture of $[tBu_4N][ReOCl_4]$ (1.8 mg, 3.0 μmol) in MeOH (250 μL). The mixture was shaken for 2.5 h, then diluted with Milli-Q water (5 mL), filtered (Millipore 0.45 μm porosity syringe filter), and purified by semiprep RP-HPLC (Column 6). The HPLC system involved isocratic elution of 77% Buffer A (0.1% TFA in $H_2O$) and 23% Buffer B (0.1% TFA in $CH_3CN$) (0.5% $min^{-1}$) and UV detection at λ 214, 220, 254, 280, and 350 nm with a flow rate of 5 mL $min^{-1}$. Fractions containing the desired compound were identified by HPLC-MS, consolidated, and lyophilized to afford a white solid (3.1 mg, 53%, assuming


DOI: 10.1021/acs.inorgchem.7b01247
*Inorg. Chem.* 2017, 56, 9725−9741

$[ReO(HL^1(cRGDfK))_2]CF_3CO_2$). HRMS (ESI$^+$) $m/z$ calc'd for $[ReC_{72}H_{101}N_{26}O_{17}S_2]^{2+}$ 926.3413, 926.3433, calc'd for $[ReC_{72}H_{102}N_{26}O_{17}S_2]^{3+}$ 617.8968, found 617.9939; RP-HPLC (Column 2, System A): $R_T$ (min) 11.0.

*[ReO(HL$^2$(cRGDfK))$_2$]$^+$*. The same procedure was used as for $[ReO(HL^1(cRGDfK))_2]^+$, except $H_2L^1$(cRGDfK) was replaced with $H_2L^2$(cRGDfK) (8.0 mg, 9.4 $\mu$mol) in MeOH (250 $\mu$L); ($t$Bu$_4$N)[ReOCl$_4$] (2.7 mg, 4.7 $\mu$mol) in MeOH (500 $\mu$L). The compound was purified by semipreparative RP-HPLC purification (Column 4) involved gradient elution of Buffer A (0.1% TFA in $H_2O$) and Buffer B (0.1% TFA in $CH_3CN$) from 0 to 20% over 20 min (1% min$^{-1}$), then 20 to 60% B to A over 40 min (0.5% min$^{-1}$) and UV detection at 214, 220, 254, 280, and 350 nm with a flow rate of 8 mL min$^{-1}$. Fractions containing the desired compound were identified by HPLC-MS, consolidated and lyophilized to afford a white solid (5.1 mg, ∼54%, assuming $[ReO(HL^2(cRGDfK))_2]CF_3CO_2$). HRMS (ESI$^+$) $m/z$ calc'd for $[ReC_{76}H_{109}N_{26}O_{17}S_2]^{2+}$ 954.3732, found 954.3715, calc'd for $[ReC_{76}H_{110}N_{26}O_{17}S_2]^{3+}$ 636.5847, found 636.5837; RP-HPLC (Column 2, System A): $R_T$ (min) 12.5.

*[ReO(HL$^3$(cRGDfK))$_2$]$^+$*. The same procedure was used as for $[ReO(HL^1(cRGDfK))_2]^+$, except $H_2L^1$(cRGDfK) was replaced with $H_2L^3$(cRGDfK) (4.0 mg, 4.6 $\mu$mol) in MeOH (200 $\mu$L), and other reagent quantities were adapted accordingly, [$t$Bu$_4$N][ReOCl$_4$] (1.3 mg, 2.3 $\mu$mol) in MeOH (200 $\mu$L). The HPLC system (Column 6) involved a linear gradient elution of Buffer A (0.1% TFA in $H_2O$) and Buffer B (0.1% TFA in $CH_3CN$) from 0 to 20% over 20 min (1% min$^{-1}$), then 20 to 60% B to A over 40 min (0.5% min$^{-1}$) and UV detection at 214, 220, 254, 280, and 350 nm with a flow rate of 8 mL min$^{-1}$. Fractions containing the desired compound were identified by HPLC-MS, consolidated, and lyophilized to afford a white solid (2.0 mg, ∼42%, assuming $[ReO(HL^3(cRGDfK))_2]CF_3CO_2$). HRMS (ESI$^+$) $m/z$ calc'd for $[ReC_{80}H_{101}N_{26}O_{17}S_2]^{2+}$ 974.3419, found 974.3711, calc'd for $[ReC_{80}H_{102}N_{26}O_{17}S_2]^{3+}$ 649.8972, found 650.0023; RP-HPLC (Column 2, System A): $R_T$ (min) 12.9.

*[ReO(HL$^1$(Tyr$^3$-Oct))$_2$]$^+$*. A solution of $H_2L^1$(Tyr$^3$-Oct) (9.0 mg, 7.1 $\mu$mol) in MeOH (50 $\mu$L) was added to a mixture of ($t$Bu$_4$N)[ReOCl$_4$] (2.1 mg, 3.5 $\mu$mol) and MeOH (100 $\mu$L). The reaction mixture was shaken vigorously for 2 h. Milli-Q water was added (4 mL) and the reaction was filtered (Millipore 0.45 $\mu$m porosity syringe filter). The compound was purified by semipreparative RP-HPLC purification (Column 6) with a gradient elution of Buffer A (0.1% TFA in $H_2O$) and Buffer B (0.1% TFA in $CH_3CN$) from 10 to 80% B to A, over 70 min (1.0% min$^{-1}$) and UV detection at $\lambda$ 214, 220, and 254 nm, with a flow rate of 5 mL min$^{-1}$. Fractions containing the desired compound were identified by HPLC-MS, consolidated, and lyophilized to afford a red, fluffy material (6.8 mg, ∼ 68%, assuming $[ReO(HL^1(Tyr^3\text{-}Oct))_2]CF_3CO_2$). ESI-MS (+) $m/z$ calc'd for $[ReC_{116}H_{148}N_{28}O_{27}S_6]^{2+}$ 1371.9470, found 1372.0024, calc'd for $[ReC_{116}H_{149}N_{28}O_{27}S_6]^{3+}$ 914.9673, found 915.0145; RP-HPLC (Column 2, System A): $R_T$ (min) 15.4.

*[ReO(HL$^2$(Tyr$^3$-Oct))$_2$]$^+$*. The same procedure was used as for $[ReO(HL^1(Tyr^3\text{-}Oct))_2]^+$, except $H_2L^1$(Tyr$^3$-Oct) was replaced with $H_2L^2$(Tyr$^3$-Oct) (8.0 mg, 6.2 $\mu$mol) in MeOH (200 $\mu$L) and other reagent quantities were adapted accordingly: ($t$Bu$_4$N)[ReOCl$_4$] (1.8 mg, 3.1 $\mu$mol) in MeOH (100 $\mu$L). The compound was purified by semipreparative RP-HPLC (Column 6) with isocratic elution of Buffer A (0.1% TFA in $H_2O$) and Buffer B (0.1% TFA in $CH_3CN$) at 38% Buffer B, over 60 min (1.0% min$^{-1}$) and UV detection at $\lambda$ 214, 220, and 254 nm, with a flow rate of 4 mL min$^{-1}$. Fractions containing the desired compound were consolidated and lyophilized to afford a red, fluffy material (5.5 mg, ∼61%, assuming $[ReO(HL^2(Tyr^3\text{-}Oct))_2]CF_3CO_2$). ESI-MS (+) $m/z$ calc'd for $[ReC_{120}H_{154}N_{28}O_{27}S_6]^{2+}$ 1399.9784, found 1399.4720, calc'd for $[ReC_{120}H_{156}N_{28}O_{27}S_6]^{3+}$ 933.6548, found 933.6460; RP-HPLC (Column 2, System A): $R_T$ (min) 16.2.

*[ReO(HL$^3$(Tyr$^3$-Oct))$_2$]$^+$*. Preloaded, resin-bound (Wang) ligand, $H_2L^3$(Tyr$^3$-Oct) (approximately 6.0 $\mu$mol), was swollen in $CH_2Cl_2$ and drained twice. Anhydrous DMF (2 × 10 mL) was added to the resin the mixture was stirred and drained. DMF (1 mL) was added to the washed resin and ($t$Bu$_4$N)-[ReOCl$_4$] (2.1 mg, 2.9 $\mu$mol) in DMF (50 $\mu$L) was added to the resin. The resin mixture was reacted for 2 h at RT. The solution was drained and the resin was washed with copious amounts of DMF (5 × 10 mL), $CH_2Cl_2$ (3 × 10 mL), and diethyl ether (10 mL). The crude material was cleaved off the resin by addition of TFA/$CH_2Cl_2$/TIPS/$H_2O$ (50:46:1:3 $v/v$) (20 mL). The mixture was shaken for 1.5 h and filtered and the filtrate sparged with a stream of $N_2$ until the red mixture had reduced to approximately 0.5 mL. Diethyl ether (2 × 10 mL) was added to the crude material, and the resulting precipitate was collected via centrifugation (3 min, 3600 rpm). The compound was purified by semipreparative RP-HPLC purification (Column 6) by gradient elution of Buffer A (0.1% TFA in $H_2O$) and Buffer B (0.1% TFA in $CH_3CN$) from 10 to 80% B to A, over 70 min (1.0% min$^{-1}$) and UV detection at $\lambda$ 214, 220, and 254 nm, with a flow rate of 4 mL min$^{-1}$. Fractions containing the desired compound were consolidated and lyophilized to afford a red, fluffy material (5.0 mg, ∼58%, assuming $[ReO(HL^3(Tyr^3\text{-}Oct))_2]CF_3CO_2$). ESI-MS (+) $m/z$ calc'd for $[ReC_{124}H_{148}N_{28}O_{27}S_6]^{2+}$ 1419.9470, found 1419.9281, calc'd for $[ReC_{124}H_{149}N_{28}O_{27}S_6]^{3+}$ 946.9673, found 946.1960; RP-HPLC (Column 2, System A): $R_T$ (min) 16.2.

*Synthesis of [$^{188}$ReO(HL$^1$(Tyr$^3$-Oct))$_2$]$^+$*. Rhenium-188 was produced from an ITG $^{188}$W/$^{188}$Re generator (ITG Isotope Technologies, Garching, Germany). Generator-produced $^{188}ReO_4^-$ (86 MBq) in aqueous sodium chloride solution (200 $\mu$L, 0.9% w/v) was added to a sealed, $N_2$-purged vial containing sodium tartrate (0.2 mg) and stannous chloride (0.1 mg) in water (400 $\mu$L), followed by heating at 80 °C for 30 min. An aliquot of this solution (50 $\mu$L) was added to a separate sealed, $N_2$-purged vial containing $H_2L^1$(Tyr$^3$-Oct) (100 $\mu$g) dissolved in water (100 $\mu$L). The reaction was left for 30 min at ambient temperature, after which an aliquot was removed for HPLC analysis, revealing that there was no reaction between $^{188}$Re and peptide. The reaction vial was then heated at 100 °C for 1 h, after which an aliquot was analyzed by HPLC (column 1, system F). Radiochemical yield: 67%, retention time of $[^{188}ReO(HL^1(Tyr^3\text{-}Oct))_2]^+$ = 11.6 min, compared to retention time of $[^{nat}ReO(HL^1(Tyr^3\text{-}Oct))_2]^+$ = 11.3 min and $H_2L^1$(Tyr$^3$-Oct) = 9.7 min.

**Synthesis of Technetium-99m Complexes.** Sodium pertechnetate, Na[$^{99m}$TcO$_4$] (1000 MBq), was eluted from a Gentech $^{99}$ Mo/$^{99m}$Tc sterile generator (Austin Health: Nuclear Medicine and Centre for PET, Australia, via ANSTO Health) as a 1.0 mL saline solution (0.9% $v/v$). A solution of $SnCl_2$ in 0.1 M HCl (0.5 mg mL$^{-1}$) was prepared and purged with nitrogen. Disodium tartrate dihydrate was dissolved in water (1


DOI: 10.1021/acs.inorgchem.7b01247
Inorg. Chem. 2017, 56, 9725−9741

mg $mL^{-1}$) in a separate evacuated vial, and a 0.5 mL aliquot was taken from both solutions and mixed together. To the solution was added $[^{99m}TcO_4]^-$ (0.1 mL in 0.9% saline, 108 MBq). The conjugated peptide, $H_2L^{1-4}$(cRGDfK) or $H_2L^{1-3}$($Tyr^3$-Oct), was dissolved in degassed Milli-Q water (1 mg $mL^{-1}$), and 100 $\mu$L of this mixture was added to the technetium solution. The sample was neutralized with $NaHCO_3$ (pH 6.5, approximately 55 $\mu$L) then filtered or allowed to react without neutralizing at ambient temperature for 30 to 120 min. The samples were filtered (Supelco, Iso-disc Filter, 4 mm x 0.45 $\mu$m). Radiochemical yields were evaluated by reverse-phase high-performance liquid chromatography (Column 7, System C).

*Stability Studies in Human Serum.* Human blood samples were centrifuged with a Heraeus Labofuge 6000 centrifuge at 3000*g* for 10 min (Heraeus, Hanau, Germany). Radioactivity readings for serum stability studies were taken with a Capintec CRC-35R dose calibrator (Capintec, New Jersey, USA) and were measured in MBq. Centrifugation of radioactive compounds was undertaken using an Eppendorf 5415 D centrifuge (Eppendorf, Hamburg, Germany). Partition coefficient data were collected with a PerkinElmer, Wizard 1470 (PerkinElmer, Massachusetts, USA) automatic $\gamma$ counter, which measured the radioactive decay of each sample in counts per minute (cpm).

For serum stability studies, blood from a healthy male (20 mL) was centrifuged (10 min, 3000 rpm) to separate blood plasma and red blood cells. The plasma was transferred to a separate vial and the red blood cells were discarded. An aliquot of plasma (0.6 mL) was added to labeled compound, $[^{99m}Tc(HL^3(Tyr^3\text{-Oct}))_2]^+$ (0.15 mL), the radioactivity was monitored and the mixture was then incubated at 37 °C. Aliquots (0.1 mL) of the mixture were removed from heating at 10 min and after 2 h. Acetonitrile (0.1 mL) was added to the serum/tracer mix to precipitate serum proteins. The suspension was shaken for 5 min and then centrifuged (5 min, 13 200 rpm). The radioactivity of the supernatant and pellet was recorded. The supernatant (20 $\mu$L) was analyzed by analytical RP-HPLC (Column 7, System C) for UV and radioactivity analysis and the pellet were washed with acetonitrile (3 × 0.1 mL), and radioactivity levels were again recorded (radioactivity levels of the pellet were negligible).

## ■ ASSOCIATED CONTENT

### Supporting Information

The Supporting Information is available free of charge on the ACS Publications website at DOI: 10.1021/acs.inorgchem.7b01247.

Representative RP-HPLC chromatograms (PDF)

### Accession Codes

CCDC 1543360 contains the supplementary crystallographic data for this paper. These data can be obtained free of charge via www.ccdc.cam.ac.uk/data_request/cif, or by emailing data_request@ccdc.cam.ac.uk, or by contacting The Cambridge Crystallographic Data Centre, 12 Union Road, Cambridge CB2 1EZ, UK; fax: +44 1223 336033.

## ■ AUTHOR INFORMATION


### Corresponding Author

*E-mail: pauld@unimelb.edu.au.

### ORCID

Michelle T. Ma: 0000-0002-3349-7346

Jonathan M. White: 0000-0002-0707-6257

Paul S. Donnelly: 0000-0001-5373-0080



### Funding

Australian Research Council FT130100204 (P.S.D.). People Programme (Marie Curie Actions) of the European Union's Seventh Framework Programme (FP7/2007−2013) under REA Grant Agreement Number 299009 (MTM). The Centre of Excellence in Medical Engineering Centre funded by the Wellcome Trust and EPSRC (WT088641/Z/09/Z), the KCL and UCL Comprehensive Cancer Imaging Centre funded by CRUK and EPSRC in association with the MRC and DoH (England), and the NIHR Biomedical Research Centre at Guy's and St Thomas' NHS Foundation Trust and King's College London.


### Notes

The authors declare no competing financial interest.

## ■ ACKNOWLEDGMENTS


Professor Jonathan R. Dilworth (University of Oxford) is acknowledged for the central role he played in the early aspects of this research. We acknowledge the generous support of Prof. Andrew M. Scott, A/Prof. Henri Tochon-Danguy, Dr. FT Lee, Nick Alexopoulos, and David Thomas of the Austin Hospital, Heidelberg, Victoria, Australia, for providing access to $^{99m}Tc$ and radiochemistry facilities. This research was supported by the Australian Research Council, FT130100204 (PSD). M.T.M. acknowledges the support of the People Programme (Marie Curie Actions) of the European Union's Seventh Framework Programme (FP7/2007-2013) under REA Grant Agreement Number 299009. This research was supported by the Centre of Excellence in Medical Engineering Centre funded by the Wellcome Trust and EPSRC (WT088641/Z/09/Z), the KCL and UCL Comprehensive Cancer Imaging Centre funded by CRUK and EPSRC in association with the MRC and DoH (England), and by the NIHR Biomedical Research Centre at Guy's and St Thomas' NHS Foundation Trust and King's College London. The views expressed are those of the authors and not necessarily those of the NHS, the NIHR or the DoH.


## ■ REFERENCES


(1) Bartholoma, M. D.; Louie, A. S.; Valliant, J. F.; Zubieta, J. Technetium and Gallium Derived Radiopharmaceuticals: Comparing and Contrasting the Chemistry of Two Important Radiometals for the Molecular Imaging Era. *Chem. Rev.* **2010**, *110*, 2903−2920.

(2) Donnelly, P. S. The role of coordination chemistry in the development of copper and rhenium radiopharmaceuticals. *Dalton Trans.* **2011**, *40*, 999−1010.

(3) Cutler, C. S.; Hennkens, H. M.; Sisay, N.; Huclier-Markai, S.; Jurisson, S. S. Radiometals for Combined Imaging and Therapy. *Chem. Rev.* **2013**, *113*, 858−883.

(4) Ramogida, C. F.; Orvig, C. Tumour targeting with radiometals for diagnosis and therapy. *Chem. Commun.* **2013**, *49*, 4720−4739.

(5) Blower, P. J. A nuclear chocolate box: the periodic table of nuclear medicine. *Dalton Trans.* **2015**, *44*, 4819−4844.

(6) Ramogida, C. F.; Orvig, C. Tumour targeting with radiometals for diagnosis and therapy. *Chem. Commun.* **2013**, *49*, 4720−4739.

(7) Pierschbacher, M. D.; Ruoslahti, E. Cell attachment activity of fibronectin can be duplicated by small synthetic fragments of the molecule. *Nature* **1984**, *309*, 30−33.

(8) Plow, E. F.; Pierschbacher, M. D.; Ruoslahti, E.; Marguerie, G. A.; Ginsberg, M. H. The effect of Arg-Gly-Asp-containing peptides on fibrinogen and von Willebrand factor binding to platelets. *Proc. Natl. Acad. Sci. U. S. A.* **1985**, *82*, 8057−8061.

(9) Pytela, R.; Pierschbacher, M. D.; Ginsberg, M. H.; Plow, E. F.; Ruoslahti, E. Platelet membrane glycoprotein IIb/IIIa: member of a




DOI: 10.1021/acs.inorgchem.7b01247
*Inorg. Chem.* 2017, 56, 9725−9741

family of Arg-Gly-Asp-specific adhesion receptors. *Science* **1986**, *231*, 1559−1562.
(10) Ruoslahti, E.; Pierschbacher, M. D. Arg-Gly-Asp: a versatile cell recognition signal. *Cell* **1986**, *44*, 517−518.
(11) Su, Z.-F.; Liu, G.; Gupta, S.; Zhu, Z.; Rusckowski, M.; Hnatowich, D. J. In Vitro and in Vivo Evaluation of a Technetium-99$^{m}$-Labeled Cyclic RGD Peptide as a Specific Marker of $\alpha_V\beta_3$ Integrin for Tumor Imaging. *Bioconjugate Chem.* **2002**, *13*, 561−570.
(12) Su, Z.-F.; He, J.; Rusckowski, M.; Hnatowich, D. J. In vitro cell studies of technetium-99$^{m}$ labeled RGD-HYNIC peptide, a comparison of tricine and EDDA as co-ligands. *Nucl. Med. Biol.* **2003**, *30*, 141−149.
(13) Decristoforo, C.; Faintuch-Linkowski, B.; Rey, A.; von Guggenberg, E.; Rupprich, M.; Hernandez-Gonzales, I.; Rodrigo, T.; Haubner, R. [$^{99m}$Tc]HYNIC-RGD for imaging integrin $\alpha_v\beta_3$ expression. *Nucl. Med. Biol.* **2006**, *33*, 945−952.
(14) Ji, S.; Zhou, Y.; Shao, G.; Liu, S. Evaluation of K(HYNIC)$_2$ as a Bifunctional Chelator for $^{99m}$Tc-Labeling of Small Biomolecules. *Bioconjugate Chem.* **2013**, *24*, 701−711.
(15) Ma, M. T.; Neels, O. C.; Denoyer, D.; Roselt, P.; Karas, J. A.; Scanlon, D. B.; White, J. M.; Hicks, R. J.; Donnelly, P. S. Gallium-68 Complex of a Macrobicyclic Cage Amine Chelator Tethered to Two Integrin-Targeting Peptides for Diagnostic Tumor Imaging. *Bioconjugate Chem.* **2011**, *22*, 2093−2103.
(16) Ma, M. T.; Donnelly, P. S. Peptide targeted copper-64 radiopharmaceuticals. *Curr. Top. Med. Chem.* **2011**, *11*, 500−520.
(17) Weckbecker, G.; Lewis, I.; Albert, R.; Schmid, H.; Hoyer, D.; Bruns, C. Opportunities in somatostatin research: Biological, chemical and therapeutic aspects. *Nat. Rev. Drug Discovery* **2003**, *2*, 999−1017.
(18) Maina, T.; Nock, B.; Nikolopoulou, A.; Sotiriou, P.; Loudos, G.; Maintas, D.; Cordopatis, P.; Chiotellis, E. [$^{99m}$Tc]demotate, a new $^{99m}$Tc-based [Tyr$^3$]-octreotate analogue for the detection of somatostatin receptor-positive tumours: synthesis and preclinical results. *Eur. J. Nucl. Med. Mol. Imaging* **2002**, *29*, 742−753.
(19) Bigott-Hennkens, H. M.; Dannoon, S. F.; Noll, S. M.; Ruthengael, V. C.; Jurisson, S. S.; Lewis, M. R. Labeling, stability and biodistribution studies of $^{99m}$Tc-cyclized Tyr$^3$-octreotate derivatives. *Nucl. Med. Biol.* **2011**, *38*, 549−555.
(20) Ahmadihosseini, H.; Abedi, J.; Ghodsi Rad, M. A.; Zakavi, S. R.; Knoll, P.; Mirzaei, S.; Sadeghi, R. Diagnostic utility of $^{99m}$Tc-EDDA-tricine-HYNIC-Tyr$^3$-octreotate SPECT for differentiation of active from inactive pulmonary tuberculosis. *Nucl. Med. Commun.* **2014**, *35*, 1262−1267.
(21) de Jong, M.; Breeman, W. A. P.; Kwekkeboom, D. J.; Valkema, R.; Krenning, E. P. Tumor Imaging and Therapy Using Radiolabeled Somatostatin Analogues. *Acc. Chem. Res.* **2009**, *42*, 873−880.
(22) Abrams, M. J.; Juweid, M.; tenKate, C. I.; Schwartz, D. A.; Hauser, M. M.; Gaul, F. E.; Fuccello, A. J.; Rubin, R. H.; Strauss, H. W.; Fischman, A. J. Technetium-99$^{m}$-Human Polyclonal IgG Radiolabeled via the Hydrazino Nicotinamide Derivative for Imaging Focal Sites of Infection in Rats. *J. Nucl. Med.* **1990**, *31*, 2022−2028.
(23) Schwartz, D. A.; Abrams, M. J.; Hauser, M. M.; Gaul, F. E.; Larsen, S. K.; Rauh, D.; Zubieta, J. A. Preparation of hydrazino-modified proteins and their use for the synthesis of technetium-99$^{m}$-protein conjugates. *Bioconjugate Chem.* **1991**, *2*, 333−336.
(24) Schwartz, D. A.; Abrams, M. J.; Hauser, M. M.; Gaul, F. E.; Larsen, S. K.; Rauh, D.; Zubieta, J. A. Preparation of hydrazino-modified proteins and their use for the synthesis of $^{99m}$Tc-protein conjugates. *Bioconjugate Chem.* **1991**, *2*, 333−336.
(25) Babich, J. W.; Solomon, H.; Pike, M. C.; Kroon, D.; Graham, W.; Abrams, M. J.; Tompkins, R. G.; Rubin, R. H.; Fischman, A. J. Technetium-99m-Labeled Hydrazino Nicotinamide Derivatized Chemotactic Peptide Analogs for Imaging Focal Sites of Bacterial Infection. *J. Nucl. Med.* **1993**, *34*, 1964−1974.
(26) Nicholson, T.; Cook, J.; Davison, A.; Rose, D. J.; Maresca, K. P.; Zubieta, J. A.; Jones, A. G. The synthesis, characterization and X-ray crystal structure of the rhenium organodiazenido, organodiazene complex [$ReCl_2(PPh_3)$ ($NNC_5H_4N$) ($HNNC_5H_4N$)]. *Inorg. Chim. Acta* **1996**, *252*, 427−430.
(27) Liu, S.; Edwards, D. S.; Looby, R. J.; Harris, A. R.; Poirier, M. J.; Barrett, J. A.; Heminway, S. J.; Carroll, T. R. Labeling a Hydrazino Nicotinamide-Modified Cyclic IIb/IIIa Receptor Antagonist with $^{99m}$Tc Using Aminocarboxylates as Coligands. *Bioconjugate Chem.* **1996**, *7*, 63−71.
(28) Hirsch-Kuchma, M.; Nicholson, T.; Davison, A.; Davis, W. M.; Jones, A. G. Synthesis and Characterization of Rhenium(III) and Technetium(III) Organohydrazide Chelate Complexes. Reactions of 2-Hydrazinopyridine with Complexes of Rhenium and Technetium. *Inorg. Chem.* **1997**, *36*, 3237−3241.
(29) King, R. C.; Surfraz, M. B.-U.; Biagini, S. C. G.; Blower, P. J.; Mather, S. J. How do HYNIC-conjugated peptides bind technetium? Insights from LC-MS and stability studies. *Dalton Trans.* **2007**, 4998−5007.
(30) Greenland, W. E. P.; Howland, K.; Hardy, J.; Fogelman, I.; Blower, P. J. Solid-phase synthesis of peptide radiopharmaceuticals using Fmoc-N-ε-(hynic-Boc)-lysine, a technetium-binding amino acid: application to Tc-99$^{m}$-labeled salmon calcitonin. *J. Med. Chem.* **2003**, *46*, 1751−1757.
(31) Dilworth, J. R. Diazene, diazenido, isodiazene and hydrazido complexes. *Coord. Chem. Rev.* **2017**, *330*, 53−94.
(32) Meszaros, L. K.; Dose, A.; Biagini, S. C. G.; Blower, P. J. Synthesis and evaluation of analogues of HYNIC as bifunctional chelators for technetium. *Dalton Trans.* **2011**, *40*, 6260−6267.
(33) Meszaros, L. K.; Dose, A.; Biagini, S. C. G.; Blower, P. J. Hydrazinonicotinic acid (HYNIC) - Coordination chemistry and applications in radiopharmaceutical chemistry. *Inorg. Chim. Acta* **2010**, *363*, 1059−1069.
(34) Liu, S.; Hsieh, W.-Y.; Kim, Y.-S.; Mohammed, S. I. Effect of Coligands on Biodistribution Characteristics of Ternary Ligand $^{99m}$Tc Complexes of a HYNIC-Conjugated Cyclic RGDfK Dimer. *Bioconjugate Chem.* **2005**, *16*, 1580−1588.
(35) Edwards, D. S.; Liu, S.; Barrett, J. A.; Harris, A. R.; Looby, R. J.; Ziegler, M. C.; Heminway, S. J.; Carroll, T. R. New and Versatile Ternary Ligand System for Technetium Radiopharmaceuticals: Water Soluble Phosphines and Tricine as Coligands in Labeling a Hydrazinonicotinamide-Modified Cyclic Glycoprotein IIb/IIIa Receptor Antagonist with $^{99m}$Tc. *Bioconjugate Chem.* **1997**, *8*, 146−154.
(36) Liu, S.; Edwards, D. S.; Harris, A. R. A Novel Ternary Ligand System for $^{99m}$Tc-Labeling of Hydrazino Nicotinamide-Modified Biologically Active Molecules Using Imine-N-Containing Heterocycles as Coligands. *Bioconjugate Chem.* **1998**, *9*, 583−595.
(37) Liu, S.; Hsieh, W.-Y.; Jiang, Y.; Kim, Y.-S.; Sreerama, S. G.; Chen, X.; Jia, B.; Wang, F. Evaluation of a $^{99m}$Tc-labeled cyclic RGD tetramer for noninvasive imaging integrin alpha(v)beta3-positive breast cancer. *Bioconjugate Chem.* **2007**, *18*, 438−446.
(38) Wang, L.; Shi, J.; Kim, Y.-S.; Zhai, S.; Jia, B.; Zhao, H.; Liu, Z.; Wang, F.; Chen, X.; Liu, S. Improving tumor-targeting capability and pharmacokinetics of $^{99m}$Tc-labeled cyclic RGD dimers with PEG(4) linkers. *Mol. Pharmaceutics* **2009**, *6*, 231−245.
(39) Jia, B.; Liu, Z.; Zhu, Z.; Shi, J.; Jin, X.; Zhao, H.; Li, F.; Liu, S.; Wang, F. Blood clearance kinetics, biodistribution, and radiation dosimetry of a kit-formulated integrin $\alpha_v\beta_3$-selective radiotracer $^{99m}$Tc-3PRGD$_2$ in non-human primates. *Mol. Imag. Biol.* **2011**, *13*, 730−736.
(40) Rose, D. J.; Maresca, K. P.; Nicholson, T.; Davison, A.; Jones, A. G.; Babich, J.; Fischman, A.; Graham, W.; DeBord, J. R. D.; Zubieta, J. Synthesis and Characterization of Organohydrazino Complexes of Technetium, Rhenium, and Molybdenum with the {M($\eta^1$-HNNR)($\eta^2$-HyNNR)} Core and Their Relationship to Radiolabeled Organohydrazine-Derivatized Chemotactic Peptides with Diagnostic Applications. *Inorg. Chem.* **1998**, *37*, 2701−2716.
(41) Kovacs, M. S.; Hein, P.; Sattarzadeh, S.; Patrick, B. O.; Emge, T. J.; Orvig, C. Complexes of phosphine-phenolate ligands with the $[ReO]^{3+}$ and $[Re(HNNC_5HN)(NNCH_4N)]^{2+}$ cores. *J. Chem. Soc., Dalton Trans.* **2001**, 3015−3024.
(42) Cowley, A. R.; Dilworth, J. R.; Donnelly, P. S. A Mono-Diazenide Complex from Perrhenate: Toward a New Core for Rhenium Radiopharmaceuticals. *Inorg. Chem.* **2003**, *42*, 929−931.


DOI: 10.1021/acs.inorgchem.7b01247
*Inorg. Chem.* 2017, 56, 9725−9741

(43) Cowley, A. R.; Dilworth, J. R.; Donnelly, P. S.; Ross, S. J. Rhenium diazenide ternary complexes with dithiocarbamate ligands: Towards new rhenium radiopharmaceuticals. *Dalton Trans.* **2007**, 73−82.
(44) Clarke, C.; Cowley, A. R.; Dilworth, J. R.; Donnelly, P. S. Pyridylthiocarbazide complexes of rhenium with potential radiopharmaceutical applications. *Dalton Trans.* **2004**, 2402−2403.
(45) Alberto, R.; Cowley, A. R.; Dilworth, J. R.; Donnelly, P. S.; Pratt, J. Diazenide and hydrazide(2-) derivatives of the $[Re(CO)_3]^+$ core. *Dalton Trans.* **2004**, 2610−2611.
(46) Torres, J. B.; Andreozzi, E. M.; Dunn, J. T.; Siddique, M.; Szanda, I.; Howlett, D. R.; Sunassee, K.; Blower, P. J. PET imaging of copper trafficking in a mouse model of Alzheimer disease. *J. Nucl. Med.* **2016**, *57*, 109−114.
(47) Teng, B.; Bai, Y.; Chang, Y.; Chen, S.; Li, Z. Technetium-99m-labeling and synthesis of thymidine analogs: Potential candidates for tumor imaging. *Bioorg. Med. Chem. Lett.* **2007**, *17*, 3440−3444.
(48) Santos, I. G.; Abram, U. Oxorhenium(V) Complexes with Thiosemicarbazones. *Z. Anorg. Allg. Chem.* **2004**, *630*, 697−700.
(49) Bandoli, G.; Gerber, T. I. A. Synthesis and characterization of tetrabutylammonium trans-bis(2-amidobenzenethiolato(2-)-S,N)-oxotechnetate(V) and its reduction by 2-aminobenzenethiol. *Inorg. Chim. Acta* **1987**, *126*, 205−208.
(50) Chi, D. Y.; Katzenellenbogen, J. A. Selective formation of heterodimeric bis-bidentate aminothiol-oxometal complexes or rhenium(V). *J. Am. Chem. Soc.* **1993**, *115*, 7045−7046.
(51) Konno, T.; Shimazaki, Y.; Kawai, M.; Hirotsu, M. Synthesis, Characterization, and Stereochemistry of Oxorhenium(V) Complexes with 2-Aminoethanethiolate. *Inorg. Chem.* **2001**, *40*, 4250−4256.
(52) Mayer, J. M. Metal-oxygen multiple bond lengths: a statistical study. *Inorg. Chem.* **1988**, *27*, 3899−3903.
(53) Nugent, W. A.; Mayer, J. M.: *Metal-Ligand Multiple Bonds: The Chemistry of Transition Metal Complexes Containing Oxo, Nitrido, Imido, Alkylidene, or Alkylidyne Ligands*; Wiley: Ann Arbor, MI, 1988.
(54) Alvarez Luna, S.; Bolzati, C.; Duatti, A.; Zucchini, G. L.; Bandoli, G.; Refosco, F. Formation of the trans-[dioxorhenium(1+)] group from the reactions of $ReNCl_2(PPh_3)_2$, $ReCl_4(PPh_3)_2$, and $ReCl_3(CH_3CN)(PPh_3)_2$ with chelating amines and tetraazamacrocycles. Crystal structure of trans-$[ReO_2(cyclam)](PF_6)$ (cyclam = 1,4,8,11-tetraazacyclotetradecane). *Inorg. Chem.* **1992**, *31*, 2595−2598.
(55) Wang, Y. P.; Che, C. M.; Wong, K. Y.; Peng, S. M. Spectroscopy, molecular structure, and electrochemistry of rhenium(V) oxo and imido complexes of 1,4,8,11-tetraazacyclotetradecane (cyclam). *Inorg. Chem.* **1993**, *32*, 5827−5832.
(56) Le Gal, J.; Tisato, F.; Bandoli, G.; Gressier, M.; Jaud, J.; Michaud, S.; Dartiguenave, M.; Benoist, E. Synthesis and structural characterization of new oxorhenium and oxotechnetium complexes with $XN_2S$-tetradentate semi-rigid ligands (X = O, S, N). *Dalton Trans.* **2005**, 3800−3807.
(57) Paterson, B. M.; White, J. M.; Donnelly, P. S. A hexadentate bis(thiosemicarbazonato) ligand: rhenium(V), iron(III) and cobalt(III) complexes. *Dalton Trans.* **2010**, *39*, 2831−2837.
(58) Cowley, A. R.; Dilworth, J. R.; Donnelly, P. S.; Woollard-Shore, J. Synthesis and characterisation of new homoleptic rhenium thiosemicarbazone complexes. *Dalton Trans.* **2003**, 748−754.
(59) Greenland, W. E. P.; Howland, K.; Hardy, J.; Fogelman, I.; Blower, P. J. Solid-Phase Synthesis of Peptide Radiopharmaceuticals Using Fmoc-N-ε-(Hynic-Boc)-Lysine, a Technetium-Binding Amino Acid: Application to Tc-99m-Labeled Salmon Calcitonin. *J. Med. Chem.* **2003**, *46*, 1751−1757.
(60) Stephenson, K. A.; Zubieta, J.; Banerjee, S. R.; Levadala, M. K.; Taggart, L.; Ryan, L.; McFarlane, N.; Boreham, D. R.; Maresca, K. P.; Babich, J. W.; Valliant, J. F. A New Strategy for the Preparation of Peptide-Targeted Radiopharmaceuticals Based on an Fmoc-Lysine-Derived Single Amino Acid Chelate (SAAC). Automated Solid-Phase Synthesis, NMR Characterization, and in Vitro Screening of fMLF(SAAC)G and fMLF[(SAAC-$Re(CO)_3)^+$]G. *Bioconjugate Chem.* **2004**, *15*, 128−136.
(61) James, S.; Maresca, K. P.; Allis, D. G.; Valliant, J. F.; Eckelman, W.; Babich, J. W.; Zubieta, J. Extension of the Single Amino Acid Chelate Concept (SAAC) to Bifunctional Biotin Analogues for Complexation of the $M(CO)_3$+1 Core (M = Tc and Re): Syntheses, Characterization, Biotinidase Stability, and Avidin Binding. *Bioconjugate Chem.* **2006**, *17*, 579−589.
(62) Maresca, K. P.; Hillier, S. M.; Femia, F. J.; Zimmerman, C. N.; Levadala, M. K.; Banerjee, S. R.; Hicks, J.; Sundararajan, C.; Valliant, J.; Zubieta, J.; Eckelman, W. C.; Joyal, J. L.; Babich, J. W. Comprehensive Radiolabeling, Stability, and Tissue Distribution Studies of Technetium-$99^m$ Single Amino Acid Chelates (SAAC). *Bioconjugate Chem.* **2009**, *20*, 1625−1633.
(63) Bartholomae, M.; Valliant, J.; Maresca, K. P.; Babich, J.; Zubieta, J. Single amino acid chelates: a strategy for the design of technetium and rhenium radiopharmaceuticals. *Chem. Commun.* **2009**, 493−512.
(64) Haubner, R.; Gratias, R.; Diefenbach, B.; Goodman, S.; Jonczyk, A.; Kessler, H. Structural and functional aspects of RGD-containing cyclic pentapeptides as highly potent and selective integrin $\alpha_v\beta_3$ antagonists. *J. Am. Chem. Soc.* **1996**, *118*, 7461−7472.
(65) Khorana, H. G. The chemistry of carbodiimides. *Chem. Rev.* **1953**, *53*, 145−166.
(66) Petersen, A. L.; Binderup, T.; Jølck, R. I.; Rasmussen, P.; Henriksen, J. R.; Pfeifer, A. K.; Kjær, A.; Andresen, T. L. Positron emission tomography evaluation of somatostatin receptor targeted $^{64}$Cu-TATE-liposomes in a human neuroendocrine carcinoma mouse model. *J. Controlled Release* **2012**, *160*, 254−263.
(67) Shi, J.; Wang, L.; Kim, Y.-S.; Zhai, S.; Liu, Z.; Chen, X.; Liu, S. Improving Tumor Uptake and Excretion Kinetics of $^{99m}$Tc-Labeled Cyclic Arginine-Glycine-Aspartic (RGD) Dimers with Triglycine Linkers. *J. Med. Chem.* **2008**, *51*, 7980−7990.
(68) Wang, L.; Shi, J.; Kim, Y.-S.; Zhai, S.; Jia, B.; Zhao, H.; Liu, Z.; Wang, F.; Chen, X.; Liu, S. Improving Tumor-Targeting Capability and Pharmacokinetics of $^{99m}$Tc-Labeled Cyclic RGD Dimers with $PEG_4$ Linkers. *Mol. Pharmaceutics* **2009**, *6*, 231−245.
(69) Liu, Z.; Jia, B.; Shi, J.; Jin, X.; Zhao, H.; Li, F.; Liu, S.; Wang, F. Tumor Uptake of the RGD Dimeric Probe $^{99m}$Tc-$G_3$-2P4-$RGD_2$ is Correlated with Integrin $\alpha_v\beta_3$ Expressed on both Tumor Cells and Neovasculature. *Bioconjugate Chem.* **2010**, *21*, 548−555.
(70) Zhou, Y.; Kim, Y.-S.; Lu, X.; Liu, S. Evaluation of $^{99m}$Tc-Labeled Cyclic RGD Dimers: Impact of Cyclic RGD Peptides and $^{99m}$Tc Chelates on Biological Properties. *Bioconjugate Chem.* **2012**, *23*, 586−595.
(71) Yang, Y.; Ji, S.; Liu, S. Impact of Multiple Negative Charges on Blood Clearance and Biodistribution Characteristics of $^{99m}$Tc-Labeled Dimeric Cyclic RGD Peptides. *Bioconjugate Chem.* **2014**, *25*, 1720−1729.
(72) Imberti, C.; Terry, S. Y. A.; Cullinane, C.; Clarke, F.; Cornish, G. H.; Ramakrishnan, N. K.; Roselt, P.; Cope, A. P.; Hicks, R. J.; Blower, P. J.; Ma, M. T. Enhancing PET Signal at Target Tissue in Vivo: Dendritic and Multimeric Tris(hydroxypyridinone) Conjugates for Molecular Imaging of $\alpha_v\beta_3$ Integrin Expression with Gallium-68. *Bioconjugate Chem.* **2017**, *28*, 481−495.
(73) Atherton, E.; Fox, H.; Harkiss, D.; Logan, C. J.; Sheppard, R. C.; Williams, B. J. A mild procedure for solid phase peptide synthesis: use of fluorenylmethoxycarbonylamino-acids. *J. Chem. Soc., Chem. Commun.* **1978**, 537−539.
(74) Sheldrick, G. M. A short history of SHELX. *Acta Crystallogr., Sect. A: Found. Crystallogr.* **2008**, *64*, 112−122.
(75) Sheldrick, G. M. Crystal structure refinement with SHELXL. *Acta Crystallogr., Sect. C: Struct. Chem.* **2015**, *71*, 3−8.
(76) Farrugia, L. J. WinGX and ORTEP for Windows: an update. *J. Appl. Crystallogr.* **2012**, *45*, 849−854.
(77) Spek, A. L. PLATON SQUEEZE: a tool for the calculation of the disordered solvent contribution to the calculated structure factors. *Acta Crystallogr., Sect. C: Struct. Chem.* **2015**, *71*, 9−18.



DOI: 10.1021/acs.inorgchem.7b01247
*Inorg. Chem.* 2017, 56, 9725−9741